TECHNICAL REPORT DOCUMENTATION PAGE

1. Report No. CA-20-3343	**2. Government Accession No.** N/A	**3. Recipient's Catalog No.** N/A
4. Title and Subtitle Congestion Reduction via Personalized Incentives		**5. Report Date** December 2020 **6. Performing Organization Code** N/A
7. Author(s) Ali Ghafelebashi, https://orcid.org/0000-0001-8339-7960 Meisam Razaviyayn, https://orcid.org/0000-0003-4342-6661 Maged Dessouky, https://orcid.org/0000-0002-9630-6201		**8. Performing Organization Report No.**
9. Performing Organization Name and Address University of Southern California, Los Angeles, CA 90089		**10. Work Unit No.** 65A0686, Task Order 3343 **11. Contract or Grant No.** USDOT Grant 69A3551747114
12. Sponsoring Agency Name and Address U.S. Department of Transportation Office of the Assistant Secretary for Research and Technology 1200 New Jersey Avenue, SE, Washington, DC 20590 California Department of Transportation Division of Research, Innovation and System Information, MS-83 1727 30th Street, Sacramento, CA 95816 USC Viterbi School of Engineering, 3650 McClintock Ave, Los Angeles, CA 90089		**13. Type of Report and Period Covered** Final Report (January 2020-December 2020) **14. Sponsoring Agency Code** USDOT OST-R
15. Supplementary Notes Dataset DOI: DOI https://doi.org/10.5061/dryad.ncjsxkst8		

16. Abstract

With rapid population growth and urban development, traffic congestion has become an inescapable issue, especially in large cities. Many congestion reduction strategies have been proposed in the past, ranging from roadway extension to transportation demand management programs. In particular, congestion pricing schemes have been used as negative reinforcements for traffic control. This project studies a different approach of offering positive incentives to drivers to take alternative routes. More specifically, an algorithm is proposed to reduce traffic congestion and improve routing efficiency by offering personalized incentives to drivers. The idea is to use the wide-accessibility of smart communication devices to communicate with drivers and develop a look-ahead incentive offering mechanism using individuals' routing preferences and aggregate traffic information. The incentives are offered after solving large-scale optimization problems in order to minimize the expected congestion (or minimize the expected carbon emission). Since these massive size optimization problems need to be solved continually in the network, a distributed computational approach is developed where a major computational burden is carried out on the individual drivers' smartphones (and in parallel among drivers). The convergence of the proposed is established distributed algorithm under a mild set of assumptions (that are verified using real data.

17. Key Words Congestion reduction, Personalized incentives, Routing, Emissions	**18. Distribution Statement** No restrictions.		
19. Security Classif. (of this report) Unclassified	**20. Security Classif. (of this page)** Unclassified	**21. No. of Pages** 60	**22. Price** N/A

NCST

About the National Center for Sustainable Transportation

The National Center for Sustainable Transportation is a consortium of leading universities committed to advancing an environmentally sustainable transportation system through cutting-edge research, direct policy engagement, and education of our future leaders. Consortium members include: University of California, Davis; University of California, Riverside; University of Southern California; California State University, Long Beach; Georgia Institute of Technology; and University of Vermont. More information can be found at: ncst.ucdavis.edu.

Disclaimer

Acknowledgments

This study was funded, partially or entirely, by a grant from the National Center for Sustainable Transportation (NCST), supported by the U.S. Department of Transportation (USDOT) and the California Department of Transportation (Caltrans) through the University Transportation Centers program. The authors would like to thank the NCST, the USDOT, and Caltrans for their support of university-based research in transportation, and especially for the funding provided in support of this project. We would like to thank Sina Baharlouei for doing peer review and report preparation, Tianjian Huang for helpful comments in simulations, Ying Peng for technical comments during the literature review, Chrysovalantis Anastasiou and Yougeng Lu for providing technical help during data extraction from the Archieved Data Management System (ADMS) system, and Pengfei Chen for technical comments in defining the emission function.

NCST

Congestion Reduction via Personalized Incentives

A National Center for Sustainable Transportation Research Report

December 2020

Ali Ghafelebashi, Daniel J. Epstein Department of Industrial & Systems Engineering, University of Southern California

Meisam Razaviyayn, Daniel J. Epstein Department of Industrial & Systems Engineering, University of Southern California

Maged Dessouky, Daniel J. Epstein Department of Industrial & Systems Engineering, University of Southern California

NCST

[page intentionally left blank]

TABLE OF CONTENTS

List of Tables

List of Figures

Congestion Reduction via Personalized Incentives

EXECUTIVE SUMMARY

Traffic congestion has become inescapable in large metropolitan areas across the world, causing huge economic losses and severely damaging the quality of life. In addition, traffic congestion leads to increased level of vehicle emissions, which is the dominant source of air pollution according to The Transportation Research Board (TRB Special Report 264). To reduce traffic congestion, various strategies have been proposed in the past decades, ranging from roadway extensions to transportation demand management programs. While many of these solutions are not feasible due to limited infrastructure investment, with the projected road demand increase, transportation planners must find ways to improve transportation conditions in a cost-efficient manner.

Recently, with advances in sensors, communication and storage technologies, significant advances have been made in the procurement and provision of real-time information that would be required for the effective control of a transportation system. Yet, the efforts based on the collected data, have had limited success to date addressing congestion in most urban cities. In addition to improved data acquisition, public access to Geo-positional System (GPS)-enabled mobile devices has significantly increased over the past decade. According to numerous market research reports, the number of U.S. adults owning smartphones have increased to more than 70%. This number even increased to 94% for young adults (Mobile Fact Sheet Report 2019). This significant user penetration level provides an opportunity to develop a platform (such as a cellphone application) to communicate with drivers in order to find efficient routing to avoid congestion. While such a platform cannot directly enforce the socially optimal routing strategy on each driver, they can influence each driver's decision by providing incentives to each driver. Such incentives could be government subsidies or incentives provided by private businesses, such as giving users' discounts to bring drivers to their business at certain times of the day. The incentives could be offered to individuals through a communication device, such as mobile cellphones when a congestion is predicted to happen in the network.

In this research, we developed a real-time (distributed) algorithm for offering personalized incentives to individual drivers to make socially optimal routing decisions. Our methodology relies on online and historical traffic data collected from various sensors/devices as well as individual preferences and routing options. Some of the key features considered in our methodology are as follows: individual's preferences and their (possible) responses to the offered incentives; route preferences due to individual safety concerns; stochastic and uncertain nature of each driver's response to the offers made; and each individual's preference among the existing set of incentives. Furthermore, our method was able to avoid creation of new congestions in other parts of the network. In our framework, there is no need for participation of the entire population and only a fraction of drivers' participation suffices. In addition, our proposed distributed algorithm has theoretical convergence guarantee under a mild set of assumptions that are verified with real data.

Finally, we will evaluated the performance of the proposed method using data from the Los Angeles area. We used the University of Southern California (USC), Archived Data Management System (ADMS) that collects, archives, and integrates a variety of transportation datasets from Los Angeles, Orange, San Bernardino, Riverside, and Ventura Counties. ADMS includes access to real-time traffic datasets from: i) 9,500 highway and arterial loop detectors providing data approximately every 1 minute, and ii) 2,500 bus and train GPS location (AVL) data operating throughout Los Angeles County. Our numerical evaluations on this data show that the proposed framework can lead up to a 27% decrease in the total carbon emission of the system during rush hour times.

Introduction

According to the Transportation Statistics Annual Report of 2018, from 2000 to 2018, the total number of registered vehicles increased by 19%, and vehicle-miles of travel increased by 15.6% [1]. However, during the same period, total lane-miles only expanded by 6% and public road and street mileage was merely augmented by 5.1% [1]. The combination of slow transportation infrastructure expansion and the growth in the number of registered vehicles have led to severe traffic congestion in urban areas. Today, traffic congestion is one of the most prevalent issues in large metropolitan areas, resulting in lowered the quality of life for residents and economic losses. According to INRIX, a company that provides traffic management services by transportation data analysis, the United States' economy suffered $88 billion in losses and United States (U.S.) drivers lost 99 hours due to traffic congestion in 2019 [2]. For instance, in Los Angeles, one of the most congested cities in the U.S., each driver lost $1524 in addition to 103 hours in 2019 due to traffic congestion [3].

In addition to direct economic losses, traffic congestion can worsen air quality and adversely affect health conditions. According to the Transportation Research Board, one of the seven program units of the National Academies of Sciences, Engineering, and Medicine, vehicle emissions are the main cause for air pollution [4]. The escalation of intensity and duration of traffic congestion can raise emissions levels [5], and as a result, air pollution (specifically NO2) increases with traffic congestion [6]. Based on the study by Hennessy and Wiesenthal, when roads are congested, drivers show aggressive behaviors more often, and their stress level rises [7]. This research shows that the Likert scale, a psychometric scale which ranges from 0 = "low stress level" to 4 = "high stress level", can increase by two times from 0.8 to 1.73 during high levels of congestion. Thus, it can increase the number of accident occurrences [8].

As possible solutions to traffic congestion, Cambridge Systematics [9] –which works on planning and policy, movement of people and goods, software design and development, and effective partnerships and objective analysis– has proposed three categories of strategies:

1) Adding more capacity;

2) Transportation System Management and Operation (TSM&O);

3) and Demand management.

The first strategy includes expanding infrastructures, such as increasing the number of available highway lanes and constructing new roads. While this strategy may result in reducing congestion[1], different reasons such as opposition from local and national groups, have made this

[1] The increase in lane miles will increase the Vehicle Miles Traveled (VMT) [94-95]. Hence, in congested metropolitan area, it is unlikely to have congestion improvement by increasing the lane miles [95]. Therefore, this

strategy very challenging in recent years. In TSM&O, the aim is to improve the efficiency of the current transportation infrastructure and manage the short-term demand for the existing network. Reversible commuter lanes, dynamic re-timing of traffic signals, providing information about travel conditions to travelers, and converting streets to one-way operations are examples of TSM&O strategies. Compared to the "adding more capacity" category, the cost of implementation in TSM&O strategies is less. While the TSM&O strategies have shown to be highly cost-effective, we cannot only rely on TSM&O strategies. The final category, Demand Management includes Travel Demand Management (TDM), non-automotive travel modes, and land use management. Travel demand management is focused on managing travel demand instead of increasing transportation infrastructure. TDM includes putting more people into fewer vehicles (e.g., ride-sharing), shifting the time of travel, and removing the need for travel altogether (e.g., teleworking). The requirement that travelers drastically change their lifestyle is one of the main obstacles of the TDM strategies. Another limitation of TDM is the inflexible schedule of workers. Investing in non-automotive modes of travels such as pedestrian infrastructure, bike-ways, and bus and rail transit systems is another strategy to decrease the rate of travel by personal vehicles.

The above strategies can be divided into two groups: (a) expanding the transportation infrastructure, and (b) increasing the efficiency of the existing network. Strategies that are based on expanding the roads need a long planning horizon before they can lessen congestion [10]. According to the U.S. Census Bureau [10] estimate, the U.S. population will grow by 28 million by 2030. If low public support for tax increases (needed to expand the transportation infrastructure) continues, innovative solutions to utilize the existing network more efficiently becomes crucial. Thus, there is an urgent need to make the existing road network more efficient.

In this research project, the focus is on changing drivers' behavior by offering incentives in order to reduce traffic congestion. More precisely, our solution lies in category 3 of the Cambridge Systematics, strategy framework: Demand Management. Perhaps the closest strategy to our solution is pricing mechanisms in the literature. Road pricing policies, such as assigning a fee or tax for driving on a highway/road, have been widely studied in theory and practice. The work of [12] and [13] study the change in drivers' behavior by imposing monetary penalties on the drivers' travel (see the book [14], Ph.D. thesis [15], and the references therein). In this category, a decline in traffic congestion is expected as a result of discouraging people to use congested roads. Such pricing mechanisms could be dependent on different factors such as time [16], distance [17], or vehicle characteristics [18].

While pricing seems a legitimate solution from a market point of view, issues such as equity barriers complicate the implementation of congestion pricing/taxation schemes [19]. In

---

study is not verified based on VMT.

particular, in some of the past implementations in Lyon, France; Mexico City, Mexico; and Genoa, Italy; congestion pricing was tested, but they failed to achieve permanent implementation due to low public acceptance [23]. In addition to equity concerns, complexity and uncertainties in designing pricing mechanisms have prevented policymakers from implementing advanced congestion pricing schemes [25]. To resolve such barriers, Gu et al. [26] proposed pricing models for a barrier area, an area in which drivers can be charged in different ways when they enter to meet efficiency and equity concerns. Their model is a joint distance and time toll. Based on this model, if a driver travels on very long routes that are not congested, they do not contribute to the traffic congestion so only the amount of time spent in the traffic jam is penalized.
Tradable credits (TCs) or tradable mobility permits (TPMs) are another token-based pricing mechanism [27]. These schemes allow certain tokens/credits to be traded among drivers through a market mechanism. The total amount of credits is typically considered constant and puts a limit on the total number of vehicles in use – see [30] for a review article on this topic. Various schemes, such as receiving free travel cards [31], have been proposed in this category. In addition, many mathematical programming approaches, such as the ones in [32] and the references therein, are proposed for the modeling and algorithms for such token-based schemes. The theoretical advantages of such tradable credits have been shown in [33]. While such cap-and-trade programs have been implemented in some economic sectors, such as airport slot allocation [37], it has not been implemented for individual-level personal travels and daily commutes [38] due to the design complexities of such token markets [39].

Lately, researchers have paid more attention to positive incentive policies. Based on the psychological theory of reactance, rewarding desirable behavior could work better than penalizing undesirable behavior [40]. Moreover, rewarding is a more popular policy than the taxation approach [40]. While the effectiveness of rewarding in changing the individual's behavior have been shown in [42] and [43], there is a limited number of studies on the effectiveness of rewarding policies in the transportation area. Among these studies, the INSTANT project [44] has provided positive incentives to motivate commuters to avoid peak times for their travel. Peak time or rush hours are the time of the day with maximum congestion. The CAPRI project of Stanford [45] is another example of peak avoidance studies using positive incentives. This study also encourages other commute modes such as walking and biking; and they have shown the effectiveness of the rewarding policy in congestion reduction. Another series of studies has been done in the Netherlands on the effectiveness of monetary rewards to avoid rush hour driving [46]. They offered incentives to the drivers to avoid rush hours (before and after the peak of the traffic in the morning), work from home, or choose alternative travel modes such as cycling, carpooling, and public transport. Xianbao et al. [49] offered different levels of incentives to alter the drivers' departure and route choices. They provided information about the travel time for each offered departure time, and alternative time, so the driver does not depend on her experience in choosing the alternatives. Recently [39] offered token form incentives for different travel choices such as route, travel modes, and ride-sharing. The proposed model learns individuals' decisions and adapts to their preferences based on their travel history. For each request, a set of choices is generated for the user and the more contribution to the network from an alternative, the more valuable incentive was offered. While these policies were successful in short-term experiments, the effectiveness of the rewarding policy in changing the behavior of

individuals does not necessarily result in permanent changes in the travelers' behavior. For example, although the effectiveness of the rewarding policy in changing the behavior of individuals was shown in [50], most of the individuals returned to their previous behavior in the absence of incentives. In this study, we use monetary incentives in our simulation model as the incentive. However, in practice, different types of incentives such as tax credits or coupons can also be utilized to change the behavior of the drivers. Our incentives are offered online through the platform (e.g. a cellphone app); hence, users who are not planning to use the road segments will not receive incentives.

There have been different choices used as the incentive in transportation studies. Fujii et al. [51] used free bus tickets as an incentive to study the changes in the frequency of traveling by bus. In a different project in Germany, to study the increase in commuting with bus, a pre-paid bus ticket was offered to college students [52]. Also, in Australia, an early bird ticket program was offered to relieve the problem of the rail overcrowding during peak hours [53]. Free WiFi and discounted tickets fare have been effective for Beijing commuters to motivate them to avoid the rush hours of the morning [54]. In the Tripod project [39], they offered token form incentives. Earned tokens depend on energy savings, and can be redeemed for goods and services at local businesses and agencies that have joined the project. In the CAPRI project [45], users of the app collected points, and they could trade 100 points for $1 or use the points to play a game in which they may lose points or gain money and points. Knockaert et al. [19] provided smartphones to their users and users could receive money for their credits or keep the smartphone after the project if they reached a sufficient amount of credits.

The preferences of the drivers can be considered by the incentive offering platform to give personalized offers. Mohan et al. [55] divided effective factors on drivers' decision into two categories of static factors and dynamic factors. The static factors, which are fixed for each person, include the number of available transportation options and the distance of nearby transit. On the other hand, the dynamic factors, which changes from travel to travel, include weather and travel purpose. They found the factors by interviews and surveys, and they concluded that with a wide range of considered factors, personalizing can be advantageous for travel assistance. Also, the drivers' preferences can be learned through interaction with the individual [[39], [56]]. Personalized incentives can be used to offer a unique alternative for each individual. The goal is to make the offer close to the individual's preferences and maximizes the contribution to the network [39] or to minimize the cost of incentives by maximizing the probability of acceptance of the alternative [56].

The rest of this report is organized as follows. Section "Problem Description" provides a description of our problem in two steps of traffic prediction and offering personalized incentives for congestion reduction. In Section "Incentive Offering Mechanism", we model our problem for two different scenarios: operating below and above the network capacity. Then to solve the second model efficiently, we propose a distributed algorithm. Results of numerical experiments for both models are presented in Section "Numerical Experiments" using data from the Los Angeles area.

Problem Description

From a game-theoretic point of view, drivers are self-interested, and their decisions may worsen traffic congestion. The goal of incentive providing mechanisms is to motivate drivers to deviate from problematic decisions in favor of congestion reduction. In this research project, we offer positive real-time personalized incentives to achieve this goal. We have two main steps in our methodology: In Step I, the traffic condition in the near future is predicted by means of the historical traffic data, and the current traffic information. In Step II, predictions are used to provide personalized incentives to drivers to take alternative routes and to avoid the creation of traffic congestion. The implementation of the proposed model could be through a smartphone app where the traffic data can be used to offer online incentives to drivers. In addition, smartphones will help the central planner to distribute the computational load for finding the optimal incentive offering strategy.

Step I: Traffic Prediction. The prediction algorithm in Step I provides the required information to distinguish between roads with probable congestion and highways with free flow in the near future. Whether a reward should be assigned to a road and how much of a reward should be considered is based on the remaining capacity in the road segments. This information comes from a prediction algorithm with relatively high accuracy and reliability. There has been a wide range of studies to predict traffic. To use the ad-hoc traffic prediction algorithms, both the performance and the compatibility of the data need to be considered. The traffic data collected by loop sensors [[57], [58]] and GPS devices [[59], [60]] has been used to predict future traffic conditions. We will use data collected by loop detectors in this work; however, other types of traffic data can be used as well. From a methodological point of view, the majority of the most recent powerful traffic prediction algorithms are based on deep learning. Ma et al. [61] have employed Convolutional Neural Network (CNN), Cui et al. [62] propose a graph convolution LSTM, and Li et al. [57] have studied Graph Neural Network combined with Convolutional Neural Network (DCRNN). In this project, we build on the DCRNN [57] framework due to its reliable performance and compatibility with our data. We have made some modifications to the algorithm in order to make prediction performance reliable across all road segments. In particular, we changed the training procedure slightly by optimizing for more conservative risk measures rather than just the average performance. The implementation of our algorithm can be downloaded from [63]. The details of our approach are presented in Appendix "Robust Traffic Flow Prediction".

Step II: Offering Personalized Incentives for Congestion Reduction. In Step II in our framework, we offer personalized incentives to the drivers to reduce congestion based on the predicted available capacity of the road network in Step I. In particular, we propose a mathematical model for the problem of offering personalized incentives to individual drivers to make socially optimal routing decisions. Our methodology relies on individual preferences and routing options which will be explained in the next section.

Incentive Offering Mechanisms

Given the current and historical data of traffic conditions and drivers' past behavior, our goal is to find the "optimal" strategy for offering incentives to individual drivers for reducing congestion in the network. To mathematically state our problem, we start by introducing some notation. A detailed example that explains our notations can be found in Appendix "An Example of the Model and Notations".

Let us model the structure of the traffic network with a directed graph $\mathcal{G} = (\mathcal{V}, \mathcal{E})$. Here $\mathcal{V}$ is the collection of all major intersections and ramps, which form the set of nodes in the graph. We use the set of edges $\mathcal{E}$ to capture the connectivity of the nodes in the graph. Two different nodes are adjacent in the graph if it is possible to directly go from one to another without passing over any other node. The direction of an edge between two nodes is based on the direction of the road from which we can go from one point to another. We also use the notation $|\mathcal{E}|$ to denote the total number of road segments/edges in our network (i.e. the cardinality of the set $\mathcal{E}$). A route is a collection of adjacent edges that starts from one node and ends in another node in the graph. We use the one-hot encoding scheme to denote the routes. In other words, a given route is represented by a vector $r \in \{0,1\}^{|\mathcal{E}|}$. Here, the kth entry of vector r is one if the kth edge is a part of route r and it is zero, otherwise.

Let $T = \{0,1,\dots,T\}$ denote the time horizon of interest assuming the system is currently at time $t = 0$. For any $t \in T$, we use the random vector $v_t \in R^{|\mathcal{E}|}$ to represent the traffic volume on different road segments of the network at time t. More precisely, the kth entry of v_t shows the total number of vehicles of road segment k at time t. Clearly, v_t is a stochastic vector and its value depends on the incentives offered. Notice that the offered incentives can change the drivers' behavior who are using the platform in the future and thus affecting the vector v_t.

We use $\mathcal{N}$ to denote the set of drivers that we can influence their behavior through offering incentives. Drivers that are included in the set $\mathcal{N}$ are currently in the system and have sent their request to the central planner (e.g. the servers dedicated to the developed cellphone application). For any driver $n \in \mathcal{N}$, let $\mathcal{R}_n \subseteq \{0,1\}^{|\mathcal{E}|}$ denote the set of possible route options for going from its origin to its destination. Let $\mathcal{I}_n$ be the set of all incentives we can offer to driver $n \in \mathcal{N}$.

We also use the binary variable $s_i^{r,n} \in \{0,1\}$ to represent the offered incentives. For any driver $n \in \mathcal{N}$ and incentive $i \in \mathcal{I}_n$, the variable $s_i^{r,n} = 1$ if incentive i is offered to driver n to take route r; and $s_i^{r,n} = 0$ otherwise.

We will also assume that we incentivize each driver with only one offer for one of their possible routes, i.e., $\sum_{r\in\mathcal{R}_n}\sum_{i\in\mathcal{I}_n} s_i^{r,n} = 1$. Given any incentive offered to the drivers, we model the decision of the drivers stochastically. In particular, we assume after offering incentives, each driver n chooses route r with a certain probability. This probability depends on the amount of incentive we offer, the route, and the driver's preferences, as described below.

The route preferences of drivers depend on different factors such as route travel time, gender, age, and particularly the (monetary) incentive provided to the drivers in our context. Such dependence can be easily learned using standard machine learning approaches in the presence of data. For example, the work [64] models the preferences of the drivers by learning the utility of the drivers and fitting the best possible model using real data. In this project, we rely on their model for our preference modeling. We simplify their model by ignoring the less predictive features and we only consider two major features which are the travel time and amount of incentive. In particular, we assume that, given incentive $i \in \mathcal{I}_n$ to driver n, the driver chooses route r with probability

$$p_i^{r,n} = P_n(\widehat{T}_r, i), \tag{1}$$

where $\widehat{T}_r$ is the estimate of the travel time for route $\boldsymbol{r}$ provided by the incentive offering platform. Notice that when drivers make their routing decisions, they do not know the exact travel time T_r for route $\boldsymbol{r}$, but instead they rely on the estimate $\widehat{T}_r$ provided by the system. Here, we make an underlying assumption that the drivers do not include their own judgement about the travel time in their decision. However, if such individual biases for drivers exist, the system can learn it over time using standard preference learning techniques.

In the next subsections, we present our model and formulation in more detail. For the convenience of the reader, the list of notations defined here and later in the manuscript is presented in Appendix "List of Notations". We have also presented our notation in a simple example in the Appendix "An Example of the Model and Notations" that can further illustrate our notation for the reader. We present our framework under two different scenarios: First, we study the case where it is possible to bring traffic flow below the network capacity (i.e., all the links operate below their capacity). As we will see, this problem leads to a mixed integer linear programming (MILP) method, which can be solved using standard optimization solvers. Then, we study the high demand scenario where there is no feasible strategy to bring the demand below the network capacity. In this case, while it is not feasible to get rid of network congestion, we aim to optimize a certain utility of the system such as reducing the expected carbon footprint of the network given the amount of available budget. This scenario will lead to a more challenging optimization problem for which we propose a distributed algorithm for solving.

Scenario I: Operating Below Network Capacity

Let us first for simplicity assume that there exists a solution that all road segments operate below the capacity. Hence, for that solution, we can assume that the travel time of each driver will be the free flow traffic. As we will see in this section, our assumption will result in a linear programming optimization problem that can be solved efficiently using standard MILP solvers. In the next section we present a formulation which relaxes this assumption.

As explained in section "Problem Description", we model the response of the drivers to the offered incentives where the acceptance probability follows a Bernoulli random variable with the preference probabilities parameter provided in equation (1). Hence, the volume vector $\mathbf{v}_t$ is a

stochastic vector which depends on the response of the drivers to the offered incentives. The expected value of this random vector is given by

$$E[v_t] = \sum_{n\in\mathcal{N}} \sum_{i\in\mathcal{I}_n} \sum_{r\in\mathcal{R}_n} s_i^{r,n} p_i^{r,n} \beta_{r,t}. \tag{2}$$

where the vector $\beta_{r,t} \in R^{|\mathbb{E}|}$ shows the probability of being at different links of the network at time $t \in N \setminus 0$, conditioned on the fact that driver n is on route r. The time dynamics and the projection of the location of each driver during the time horizon is captured by the vector $\beta_{r,t}$. For more details about vector $\beta_{r,t}$, please refer to [65] and the example provided in Appendix "An Example of the Model and Notations".

Our goal is to minimize the cost of offering incentives while keeping the volume below the road segment capacity vector $\mathbf{v}_0$. More precisely,

$$\begin{aligned}
\min_{\{s_i^{\mathbf{r},n}\}} \quad & \sum_{n\in\mathcal{N}} \sum_{r\in\mathcal{R}_n} \sum_{i\in\mathcal{I}_n} s_i^{\mathbf{r},n} q_i \\
\text{s.t.} \quad & \mathbf{v}_t \le \mathbf{v}_0, \quad \forall t \in \mathbf{T}, \quad \text{with high probability} \\
& \sum_{\mathbf{r}\in\mathcal{R}_n} \sum_{i\in\mathcal{I}_n} s_i^{\mathbf{r},n} = 1, \quad \forall n \in \mathcal{N}, \\
& s_i^{\mathbf{r},n} \in \{0,1\}, \quad \forall n \in \mathcal{N}, \forall i \in \mathcal{I}_n, \forall \mathbf{r} \in \mathcal{R}_n
\end{aligned}$$

where q_i is the cost of offering incentive i. Here, the term "with high probability" is used to emphasize the random nature of vector v_t. This constraint can mathematically be translated to $P(v_t \le v_0, \forall t \in T) \ge \zeta$, for some given confidence level ζ. To keep this optimization problem tractable, we rely on the assumption of large number of vehicles in each road segment and approximate the random quantity v_t with its average $E[v_t]$ provided in equation (2). More precisely, we aim at solving

$$\begin{aligned}
\min_{\{s_i^{\mathbf{r},n}\}} \quad & \sum_{n\in\mathcal{N}} \sum_{r\in\mathcal{R}_n} \sum_{i\in\mathcal{I}_n} s_i^{\mathbf{r},n} q_i \\
\text{s.t.} \quad & \sum_{n\in\mathcal{N}} \sum_{i\in\mathcal{I}_n} \sum_{\mathbf{r}\in\mathcal{R}_n} s_i^{\mathbf{r},n} p_i^{\mathbf{r},n} \beta_{\mathbf{r},t} \le \mathbf{v}_0, \quad \forall t \in \mathbf{T} \\
& \sum_{\mathbf{r}\in\mathcal{R}_n} \sum_{i\in\mathcal{I}_n} s_i^{\mathbf{r},n} = 1, \quad \forall n \in \mathcal{N}, \\
& s_i^{\mathbf{r},n} \in \{0,1\}, \quad \forall n \in \mathcal{N}, \forall i \in \mathcal{I}_n, \forall \mathbf{r} \in \mathcal{R}_n
\end{aligned} \tag{3}$$

which is a mixed-integer linear programming model and can be solved with standard optimization software packages.

A natural alternative formulation in this scenario is to minimize a utility of the system subject to budget and capacity constraints. For example, we can minimize the expected value of total travel time of the drivers subject to budget and capacity constraints

$$
\begin{aligned}
\min_{\{s_i^{\mathbf{r},n}\}} \quad & \sum_{t\in\mathbf{T}} \sum_{n\in\mathcal{N}} \sum_{r\in\mathcal{R}_n} \sum_{i\in\mathcal{I}_n} s_i^{\mathbf{r},n} p_i^{\mathbf{r},n} \boldsymbol{\beta}_{\mathbf{r},t}^{\intercal} \omega \\
\text{s.t.} \quad & \sum_{n\in\mathcal{N}} \sum_{i\in\mathcal{I}_n} \sum_{\mathbf{r}\in\mathcal{R}_n} s_i^{\mathbf{r},n} p_i^{\mathbf{r},n} \boldsymbol{\beta}_{\mathbf{r},t} \leq \mathbf{v}_0, \quad \forall t \in \mathbf{T} \\
& \sum_{n\in\mathcal{N}} \sum_{i\in\mathcal{I}_n} \sum_{\mathbf{r}\in\mathcal{R}_n} s_i^{\mathbf{r},n} q_i^n \leq \Omega \\
& \sum_{\mathbf{r}\in\mathcal{R}_n} \sum_{i\in\mathcal{I}_n} s_i^{\mathbf{r},n} = 1 \quad \forall n \in \mathcal{N} \\
& s_i^{\mathbf{r},n} \in \{0,1\} \quad \forall n \in \mathcal{N}, \forall i \in \mathcal{I}_n, \forall \mathbf{r} \in \mathcal{R}_n
\end{aligned}
\tag{4}
$$

where $\omega \in R^{|\mathbb{E}|}$ is the vector of free flow travel time of the links and Ω is the total available budget. Notice that the objective function is equal to

$$
\min_{\{s_i^{\mathbf{r},n}\}} \sum_{n\in\mathcal{N}} \sum_{r\in\mathcal{R}_n} \sum_{i\in\mathcal{I}_n} s_i^{\mathbf{r},n} p_i^{\mathbf{r},n} \sum_{t\in\mathbf{T}} \boldsymbol{\beta}_{\mathbf{r},t}^{\intercal} \omega
$$

in which $\sum_{t\in T} \beta_{r,t}^{\intercal}\, \omega$ is the expected travel time of driver n on route r.

Scenario II: Operating Above Network Capacity

In this subsection, we study the scenario of operating above network capacity. In other words, we assume that the demand is elevated and; thus, there is no incentive offering strategy that will bring the traffic flow below the network capacity. In such a scenario, we still can "improve" the congestion via providing incentives to individual drivers. Our goal is to optimize a utility of the system as a criterion to compare the traffic condition after incentivizing. To make the formulation more specific, we use an environmental factor, Carbon emission, as the utility function to evaluate the improvement of traffic conditions. It is worth noting that while we use this utility in our formulation, following our steps, one can use other utility functions as the objective function.

To model and quantify the amount of emission, resulting from congestion, we rely on the ARTEMIS research program [66] that provides emission functions for CO_2 (Carbon dioxide), CO (Carbon monoxide), HC (Hydrocarbons), PM (Exhaust particulate matter), NO_x (Nitrogen Oxides) [66]. We use CO_2 emissions as our criterion to quantify the adverse impact of congestion on the environment because global warming by the late 21st century and beyond is mostly influenced by CO_2 emissions [67]. In ARTEMIS research project, CO_2 emissions are estimated via a polynomial function where the parameters and the order of the function depend on the fuel type of the engine and the emission standard of the fuel. For example, if the drivers' vehicles have Euro IV petrol engine, we have the following emission function:

$$f_{CE}(\delta) = 523.7 - (1654.4 \times 10^{-2})\,\delta + (2635.4 \times 10^{-4})\,\delta^2 - (1771.5 \times 10^{-6})\,\delta^3 + (442.9 \times 10^{-8})\,\delta^4, \quad (5)$$

where $\delta \in R$ is the average speed in km/h of the link. The output of the function is the emission factor in g/km. To compute the total CO_2 emissions at the link in grams, we need to multiply the emission factor $f_{CE}(.)$ by the length of the link in km, i.e.,

$$CO_2 \text{ emission in grams for one vehicle for traveling on a given link} = f_{CE}(\delta)L,$$

where L is the length of the link in km. Thus, one can estimate the total CO_2 emissions by a vehicle in this scenario.[2]

To compute the total Carbon emission (CO_2) of the system, we need to sum up the Carbon emissions of all links over all time periods, i.e.,

$$F_{CE}(\hat{\mathbf{v}}) = \sum_{\ell=1}^{|\mathcal{E}|} \sum_{t=1}^{|\mathrm{T}|} \hat{v}_{\ell,t} f_{CE}(\delta_{\ell,t}(\hat{\mathbf{v}}))L_\ell \quad (6)$$

where $\delta_{\ell,t}$ is the speed of link ℓ at time t (which itself is a function of the volume). Here, $\hat{v}$ is the vector of the volume of the links at different times in the horizon in which $\hat{v}_{\ell,t}$ is the $(|\ell| \times t + 1)^{th}$ element of the vector $\hat{v}$ representing the volume of the ℓ^{th} link at time t, and L_1 is the length of the ℓ^{th} link.

To understand the impact of our offered incentives to the total carbon emissions, we estimate the drivers' decision based on the provided incentives, which in turn results in estimating the volume of the links in the horizon of interest. Given these estimated volume values, we estimate the speed of the links as described below.

Speed value δ: The function $f_{CE}(\cdot)$ takes the average speed of the link as the input argument but we have access to the volume. There are different functions that capture the relation between speed and volume. For example, the link congestion function developed by the Bureau of Public Roads (BPR) [68] defines a nonlinear relation between the volume and travel time of the road segments:

$$f_{BPR}(v) = t_0\left(1 + 0.15\left(\frac{v}{w}\right)^4\right)$$

[2] Although we assume Euro IV petrol engine for all cars in the network here, one can personalize this to any individual vehicle and use the specific vehicle properties to compute the carbon emission. In other words, we can have a customized function for each car/driver in our model.

where $f_{BPR}(v)$ is the travel time of the drivers on the link given the assigned traffic volume v; the parameter t_0 is the free flow travel time of the link; v is the assigned traffic volume of the link; and w is the practical capacity of the link. We learn t_0 and w by using gradient descent and historical traffic data. We can compute the speed by rewriting the BPR function as:

$$\delta(v) = \frac{L}{f_{BPR}(v)} = \frac{L}{t_0}\left(1 + 0.15\left(\frac{v}{w}\right)^4\right)^{-1}$$

So we can rewrite the function in (6) based on the speed function $\delta(\cdot)$ as:

$$\begin{aligned} F_{CE}(\hat{\mathbf{v}}) &= \sum_{\ell=1}^{|\mathcal{E}|}\sum_{t=1}^{|\mathbf{T}|} \hat{v}_{\ell,t} f_{CE}(\delta_{\ell,t}) L_\ell \\ &= \sum_{\ell=1}^{|\mathcal{E}|}\sum_{t=1}^{|\mathbf{T}|} \hat{v}_{\ell,t} f_{CE}(\delta(v_{\ell,t})) L_\ell. \end{aligned} \tag{7}$$

Thus, in order to estimate the Carbon emissions of the system, we need to estimate the volume vector $\hat{v}$, which we discuss next.

Volume vector $\hat{v}$: To compute the volume vector, we need to know the routing decision of the drivers to be able to (approximately) estimate their location at different times. Clearly, the drivers' decision is a function of the offered incentives. In other words, the location of a driver is dependent on the incentive that we assign to them, because the likelihood of various decisions changes with different incentives. Let us first explain our notation for the offered incentives: For each driver, we have a one hot encoded vector describing which route has been incentivized and how much reward has been assigned to it. Thus, for each driver we have a binary vector $s \in \{0,1\}^{|\mathcal{R}|\cdot|\mathcal{I}|}$ in which only one element has a value of one and it corresponds to the route and the incentive amount that we offer. As we need one vector for each driver, we can aggregate all our incentivization strategy in a matrix $\boldsymbol{S} \in \{0,1\}^{(|\mathcal{R}|\cdot|\mathcal{I}|)\times|\mathcal{N}|}$. Naturally, routes that are not relevant to that OD pair of a driver will get a value of zero in the corresponding incentive vector (since we cannot offer those routes to the driver).

Using the above definition, the product $\mathbf{S1}$ is a $(|\mathcal{R}| \cdot |\mathcal{I}|) \times 1$ vector where $(\mathbf{S1})_{ri}$ represents the number of drivers receiving incentive i for choosing route r. To understand the drivers' responses to our offered incentives, we need to estimate the probability of acceptance of incentivized routes under different incentives including zero incentive (i.e, no incentive). To model this probability, we use the utility function provided in [64] and compute the probability of acceptance of each offered incentive (by using a Softmax function on top of the utility). While the model in [64] takes many parameters (such as gender, age, length of the route, education of the driver) as input, in our model and numerical experiments we only consider the travel time

and the reward value to generate the probability of acceptance of a given incentive/reward[3]. Let $\boldsymbol{P} \in [0,1]^{|\mathcal{R}|\times(|\mathcal{R}|\cdot|\mathcal{I}|)}$ be a matrix encoding the information of probability of picking different routes given the offered (route,incentive) pairs. Thus, the vector $\mathbf{PS1} \in R^{|\mathbb{R}|\times\mathbb{1}}$ shows the expected number of vehicles in each route.

Given the number of vehicles in each route, the position of each driver for the next time horizon can be modeled in a probabilistic fashion. In other words, one can model/compute the probability of the presence of a vehicle in different road segments in the next time horizon. For this purpose, we rely on the model developed in [65] where a specific matrix $\mathbf{R} \in [0,1]^{(|\mathcal{E}|\cdot|\mathcal{T}|)\times|\mathcal{R}|}$ is proposed to estimate the probability of the presence of a driver in a given road segment at a specific time in the future (assuming that the driver is picking a specific route). Thus, the vector

$$\hat{v} = \boldsymbol{RPS1} \in \mathbb{R}^{(|\mathcal{E}|\cdot|\mathcal{T}|)\times 1}$$

represents the expected number of vehicles in all the links at each time slot. Plugging in the above volume vector in the function in (7), we get:

$$\begin{aligned} F_{CE}(\hat{\mathbf{v}}) &= \sum_{\ell=1}^{|\mathcal{E}|}\sum_{t=1}^{|\mathbf{T}|} \hat{v}_{\ell,t} f_{CE}(\delta_{\ell,t}) L_\ell \\ &= \sum_{\ell=1}^{|\mathcal{E}|}\sum_{t=1}^{|\mathbf{T}|} (\mathbf{AS1})_{\ell,t} f_{CE}\left(\delta((\mathbf{AS1})_{\ell,t})\right) L_\ell \\ &= \sum_{\ell=1}^{|\mathcal{E}|}\sum_{t=1}^{|\mathbf{T}|} (\mathbf{a}_{\ell,t}\mathbf{S1}) f_{CE}\left(\delta((\mathbf{a}_{\ell,t}\mathbf{S1})_{\ell,t})\right) L_\ell \end{aligned}$$

where $a_{l,t}$ is the row of matrix $\mathbf{A} = \mathbf{RP}$ which corresponds to link l at time t. Thus in order to minimize the total Carbon emission in the system via providing incentives to drivers, we need to solve the following optimization problem:

[3] Clearly, one can make the model more accurate and personalized by including parameters such as the gender, age, and education of any individual driver.

$$
\begin{aligned}
\min_{\mathbf{S}} \quad & \sum_{\ell=1}^{|\mathcal{E}|} \sum_{t=1}^{|\mathbf{T}|} (\mathbf{a}_{\ell,t}\mathbf{S1}) f_{CE}\left(\delta((\mathbf{a}_{\ell,t}\mathbf{S1})_{\ell,t})\right) L_{\ell} \\
\text{s.t.} \quad & \mathbf{S}^{\intercal}\mathbf{1} = \mathbf{1} \\
& \mathbf{c}^{\intercal}\mathbf{S1} \leq \Omega \\
& \mathbf{DS1} = \mathbf{q} \\
& \mathbf{S} \in \{0,1\}^{(|\mathcal{R}||\mathcal{I}|)\times|\mathcal{N}|}
\end{aligned}
\tag{8}
$$

where $\mathbf{c} \in R_{+}^{|\mathbb{R}|\cdot|\mathbb{I}|}$ is the vector of cost of incentives assigned to each route, $\mathbf{D} \in \{0,1\}^{K\times(k|\mathcal{J}|)}$ is the matrix of incentive assignments to the OD pairs, and $\mathbf{q} \in R^{K\times|\mathcal{J}|}$ is the vector of the number of drivers for each OD pair. Here, K is the number of OD pairs. In what follows, we explain the constraints in more details:

Constraint 1 ($S^{\intercal}1 = \mathbf{1}$): This constraint simply states that we only assign one incentive to each driver.

Constraint 2 ($c^{\intercal}\,S\;\mathbf{1} \leq \Omega$): This is our budget constraint. We need a vector $\mathbf{c} \in R^{|\mathbb{R}|\cdot|\mathbb{I}|}$ that represents the cost of the different rewards assigned to each driver. Hence, given a matrix $\mathbf{S}$, the total cost of incentive strategy $\mathbf{S}$ can be computed as $\boldsymbol{c}^{\intercal}\boldsymbol{S}\mathbf{1}$.

Constraint 3 ($\mathbf{DS1} = q$): This constraint makes the model aware of the number of drivers that are traveling between each OD pair to make sure that we offer the correct number of rewards for the routes between each OD pair. Recall that $\mathbf{S1}$ represents the (expected) number of drivers that have been offered different routes given different rewards. We use matrix $\mathbf{D}$ to sum up the number of drivers that have received the different reward offers for the routes between the same OD pair so we get the vector of the number of drivers that are traveliing between each OD pair. $\mathbf{q}$ is the vector of the actual number of drivers that are travelling between OD pairs and $\mathbf{DS1}$ should be equal to $\mathbf{q}$.

Constraint 4 ($\mathbf{S} \in \{0,1\}^{(|\mathcal{R}||\mathcal{J}|)\times|\mathcal{N}|}$): This constraint imposes binary structure on our decision parameters. In other words, 0 is not choosing an incentive and 1 is selecting the incentive as explained before.

To better understand our model, we provide an example in Appendix "An Example of the Model and Notations".

Algorithm for Offering Incentives and A Distributed Implementation

Optimization problem (8) is of large size while it needs to be solved in real time in the network. However, due to the existence of binary variable $\mathbf{S}$, solving this problem efficiently is difficult[4]. In order to develop an efficient solver for (8), we first relax the binary constraint in (8) and replace it with the relaxed convex constraint $\mathbf{S} \in [0,1]^{(|\mathcal{R}||\mathcal{I}|)\times|\mathcal{N}|}$, leading to the relaxed formulation:

$$\begin{aligned} \min_{\mathbf{S}} \quad & \sum_{\ell=1}^{|\mathcal{E}|}\sum_{t=1}^{|\mathbf{T}|}(\mathbf{a}_{\ell,t}\mathbf{S1})\, f_{CE}\left(\delta(\mathbf{a}_{\ell,t}\mathbf{S1})\right) L_\ell \\ \text{s.t.} \quad & \mathbf{S}^\intercal\mathbf{1} = \mathbf{1} \\ & \mathbf{c}^\intercal\mathbf{S1} \leq \Omega \\ & \mathbf{DS1} = \mathbf{q} \\ & \mathbf{S} \in [0,1]^{(|\mathcal{R}||\mathcal{I}|)\times|\mathcal{N}|} \end{aligned} \tag{9}$$

The constraints in the above optimization problem are clearly convex. However, as we show in Appendix "Convexity of the CO2 Emission Function", the objective function is not necessarily convex in general. Luckily, as we demonstrate in Appendix "Convexity of the CO2 Emission Function" the above problem is convex for a wide range of problem instances and in particular for the setting of our numerical experiments. This convexity will allow us to explore the use of standard solvers such as CVX [69], a package for specifying and solving convex programs. However, these solvers rely on methods such as interior point methods [70] which requires $O(n^3)$ number of iterations with n being the number of variables. This heavy computational complexity prevents us from applying standard solvers. However, in our context, each driver is equipped with a smartphone and; thus, we can distribute the computational burden of solving (9) among the drivers. In what follows, we propose a simple reformulation of the problem leading to a distributed algorithm for solving (9).

To present our algorithm, let us start by reformulating (9) as

[4] We conjecture that problem (8) is NP-hard to solve since it is a special instance of polynomial optimization with discrete variables and there seems to be no special structure in function f to reduce its complexity.

$$
\begin{aligned}
\min_{\boldsymbol{\gamma},\mathbf{u},\mathbf{S},\mathbf{W},\mathbf{H},\mathbf{z},\beta} \quad & \sum_{\ell=1}^{|\mathcal{E}|}\sum_{t=1}^{|\mathbf{T}|}\gamma_{\ell,t} f_{CE}\left(\delta(\gamma_{\ell,t})\right) L_\ell \\
\text{s.t.} \quad & \mathbf{S1} = \mathbf{u}, \quad \mathbf{W}^\intercal \mathbf{1} = \mathbf{1} \\
& \mathbf{Du} = \mathbf{q}, \quad \mathbf{Au} = \boldsymbol{\gamma} \\
& \mathbf{H} = \mathbf{S}, \quad \mathbf{W} = \mathbf{S} \\
& \mathbf{c}^\intercal \mathbf{u} + \beta = \Omega, \quad \beta \geq 0 \\
& \mathbf{H} \in [0,1]^{(|\mathcal{R}|\cdot|\mathcal{I}|)\times|\mathcal{N}|}
\end{aligned}
\tag{10}
$$

As we discuss in Appendix "Details of Alternating Direction Method of Multipliers (ADMM)", this formulation is amenable to the ADMM method [[71]–[74]], which has a natural distributed implementation. Thus, we rely on the ADMM algorithm for solving (9). The steps of this algorithm are summarized in Algorithm 1 below and the details of the derivation of its steps is provided in Appendix "Details of Alternating Direction Method of Multipliers (ADMM)".

In Algorithm 1, $\Pi(\cdot)_{[0,1]}$ is the operator that projects each entry of the input matrix to the interval $[0,1]$. Notice that in Algorithm 1, Steps 4, 5, and 7 are computationally cumbersome due to the size of matrices $\mathbf{W}, \mathbf{S}$, and $\mathbf{H}$. However, notice that each column of the matrices $\mathbf{W}, \mathbf{S}$, and $\mathbf{H}$ corresponds to a single driver and hence the computation corresponding to each column can be performed in parallel on the smartphone devices of the drivers. Moreover, in Step 7 of Algorithm 1, we need to solve $L \times T$ single dimensional optimization problems (which we can rely on methods such as bisection or Newton to solve). Moreover, since these optimization problems are not coupled, they can be solved in parallel on the driver's smart devices. Theorem 1 guarantees the convergence of our ADMM algorithm.

Theorem 1 *Let $F_{CE}(.)$ be as defined in* (5)*. Then, Algorithm 1 finds an E-optimal solution of problem* (9) *in $O(1/E)$ iterations.*

While Algorithm 1 returns the solution of the optimization problem (9), this problem is a relaxation of the original problem (8). Hence, the obtained solution in Algorithm 1 must be "rounded" to a feasible point in (8). For this step, we use the Quantized-Alternating Direction Method of Multipliers (ADMM-Q), which has been tremendously successful in recent years for training binarized neural networks [[75]–[84]] and has been shown to converge to a "stationary" notion of the original problem in [85]. The details of this rounding process is presented in Appendix "Details of Alternating Direction Method of Multipliers (ADMM)".

Algorithm 1 ADMM

Input: Initial values: γ^0, $\mathbf{S}^0$, $\mathbf{H}^0$, $\mathbf{W}^0$, $\mathbf{u}^0$, β^0, $\boldsymbol{\lambda}_1^0 \in \mathbb{R}^{|\mathcal{R}|\cdot|\mathcal{I}|\times 1}$, $\boldsymbol{\lambda}_2^0 \in \mathbb{R}^{|\mathcal{N}|\times 1}$, $\boldsymbol{\lambda}_3^0 \in \mathbb{R}^{K\times 1}$, $\boldsymbol{\lambda}_4^0 \in \mathbb{R}^{|\mathcal{E}|\cdot\mathbf{T}\times 1}$, $\boldsymbol{\Lambda}_5^0 \in \mathbb{R}^{|\mathcal{R}|\cdot|\mathcal{I}|\times|\mathcal{N}|}$, $\lambda_6^0 \in \mathbb{R}$, $\boldsymbol{\Lambda}_7^0 \in \mathbb{R}^{|\mathcal{R}|\cdot|\mathcal{I}|\times|\mathcal{N}|}$, Dual update step: ρ, Number of iterations: T.
for $t = 0, 1, \ldots, T$ **do**
  $\mathbf{u}^{t+1} = (\rho\mathbf{I} + \rho\mathbf{D}^\intercal\mathbf{D} + \rho\mathbf{A}^\intercal\mathbf{A} + \rho\mathbf{c}\mathbf{c}^\intercal)^{-1}(\boldsymbol{\lambda}_1^t + \rho\mathbf{S}^t\mathbf{1} - \mathbf{D}^\intercal\boldsymbol{\lambda}_3^t + \rho\mathbf{D}^\intercal\mathbf{q} - \mathbf{A}^\intercal\boldsymbol{\lambda}_4^t + \rho\mathbf{A}^\intercal\boldsymbol{\gamma}^t - \mathbf{c}(\lambda_6^t + \beta^t - \Omega))$
  $\mathbf{W}^{t+1} = (\rho\mathbf{1}\mathbf{1}^\intercal + \rho\mathbf{I})^{-1}(\rho\mathbf{1}\mathbf{1}^\intercal + \rho\mathbf{S}^t - \boldsymbol{\Lambda}_7^t - \mathbf{1}\boldsymbol{\lambda}_2^{t\intercal})$
  $\mathbf{H}^{t+1} = \Pi\left(\mathbf{S}^t - \frac{1}{\rho}\boldsymbol{\Lambda}_5^t\right)_{[0,1]}$
  $\mathbf{S}^{t+1} = (\rho\mathbf{u}^{t+1}\mathbf{1}^\intercal + \boldsymbol{\Lambda}_5^t + \rho\mathbf{H}^{t+1} + \boldsymbol{\Lambda}_7^t + \rho\mathbf{W}^{t+1} - \boldsymbol{\lambda}_1^t\mathbf{1}^\intercal)(\rho\mathbf{1}\mathbf{1}^\intercal + 2\rho\mathbf{I})^{-1}$
  for $\ell = 0, 1, \ldots, |\mathcal{E}|$ **do**
    for $\hat{t} = 1, \ldots, |\mathbf{T}|$ **do**
      $\boldsymbol{\gamma}_{\ell,\hat{t}}^{t+1} = \underset{\boldsymbol{\gamma}_{\ell,\hat{t}}}{\operatorname{argmin}} \boldsymbol{\gamma}_{\ell,\hat{t}} f_{CE}\left(\delta(\boldsymbol{\gamma}_{\ell,\hat{t}})\right) L_\ell + \boldsymbol{\lambda}_{4,(\ell,\hat{t})}^t(\mathbf{a}_{\ell,\hat{t}}\mathbf{u}^t - \boldsymbol{\gamma}_{\ell,\hat{t}}) + \frac{\rho}{2}(\mathbf{a}_{\ell,\hat{t}}\mathbf{u}^t - \boldsymbol{\gamma}_{\ell,\hat{t}})^2$
    end for
  end for
  $\beta^{t+1} = \Pi\left(\Omega - \mathbf{c}^\intercal\mathbf{u}^{t+1} - \frac{1}{\rho}\lambda_6^t\right)_{\mathbb{R}_+}$
  $\boldsymbol{\lambda}_1^{t+1} = \boldsymbol{\lambda}_1^t + \rho(\mathbf{S}^{t+1}\mathbf{1} - \mathbf{u}^{t+1})$
  $\boldsymbol{\lambda}_2^{t+1} = \boldsymbol{\lambda}_2^t + \rho(\mathbf{W}^{t+1\intercal}\mathbf{1} - \mathbf{1})$
  $\boldsymbol{\lambda}_3^{t+1} = \boldsymbol{\lambda}_3^t + \rho(\mathbf{D}\mathbf{u}^{t+1} - \mathbf{q})$
  $\boldsymbol{\lambda}_4^{t+1} = \boldsymbol{\lambda}_4^t + \rho(\mathbf{A}\mathbf{u}^{t+1} - \boldsymbol{\gamma}^{t+1})$
  $\boldsymbol{\Lambda}_5^{t+1} = \boldsymbol{\Lambda}_5^t + \rho(\mathbf{H}^{t+1} - \mathbf{S}^{t+1})$
  $\lambda_6^{t+1} = \lambda_6^t + \rho(\mathbf{c}^\intercal\mathbf{u}^{t+1} + \beta^{t+1} - \Omega)$
  $\boldsymbol{\Lambda}_7^{t+1} = \boldsymbol{\Lambda}_7^t + \rho(\mathbf{W}^{t+1} - \mathbf{S}^{t+1})$
end for
Return: $\mathbf{S}^T$

Numerical Experiments

We evaluate the performance of our method using data from the Los Angeles area. The Los Angeles region is ideally suited for being the validation area because for various OD pairs, there are a number of routes that connect them. Additionally, researchers at the University of Southern California have developed the Archived Data Management System (ADMS) that collects, archives, and integrates a variety of transportation datasets from Los Angeles, Orange, San Bernardino, Riverside, and Ventura Counties. ADMS includes access to real-time traffic datasets from 9500 highway and arterial loop detectors providing data approximately every 1 minute.

Due to a lack of access to all the drivers' routing information, we need to estimate the origin-destination (OD) matrix from the network flow information. Rows and columns of the OD matrix correspond to the origin and destination points respectively. For instance, for OD matrix *A*, the element *A*(*i,j*) is the number of drivers going from point *i* to point *j*. The fundamental challenge of the OD matrix estimation problem is that it is severely under-determined [[86]–[88]]. There are two categories of OD matrices; static and dynamic OD matrix and both have been studied extensively (see the review article [89], and the references therein). In static methods, the traffic flows are considered as time-independent and an average OD demand is determined for long-term transportation planning and design purposes [89]. Dynamic OD demand represents the number of travelers departing from an origin at a particular time interval heading for a destination [65]. Due to the high resolution of our data, most of the existing dynamic OD estimation (DODE) methods become computationally inefficient. In addition, we do not have

prior data of the OD matrix which many studies consider as given data [[90]–[93]] and we do not have access to prior observations of the OD matrix. Given these barriers, we use the algorithm proposed by [65] which can handle the high-resolution data to carry out the DODE without employing any prior OD matrix information as a ground-truth.

We use CO_2 emission as one criterion to evaluate the performance of our incentive offering mechanism. We compare the performance of incentive offering mechanism to the "baseline" mechanism where no rewards are offered to the drivers.

We make the following two assumptions about the vehicles in the traffic.

- Drivers' vehicles have Petrol engine.
- The provided Petrol is Euro IV.

Based on these two assumptions, we have the following emission function:

$$f_{CE}(\delta) = 523.7 - (1654.4 \times 10^{-2})\,\delta + (2635.4 \times 10^{-4})\,\delta^2 - (1771.5 \times 10^{-6})\,\delta^3 + (442.9 \times 10^{-8})\,\delta^4$$

where $\delta \in \mathrm{R}$ is the average speed in km/h at the link.

Simulation Model

In our numerical experiments, we integrate different data sets and models to simulate our provided optimization models. First, we extract the speed data, volume data, and sensor information including the location of sensors from the Archived Data Management System (ADMS). ADMS collects, archives, and integrates a variety of transportation datasets, and it includes real-time traffic data (such as speed and volume) of arterial ways for every 1 minute. We also use distance of sensors which is extracted from the location of sensors by using Google Maps API. Using this distance data, we create the graph of the network. We created two sets of graph networks for the University of Southern California (USC) neighborhood data with two different sets of OD points which are depicted in Figure 1 and Figure 3. In the next step, the speed data, volume data, and the network graph are used for estimating OD pairs by the algorithm provided in [65]. The total number of estimated incoming drivers are presented in Figure 2 and Figure 4. For each OD pair, we find up to four different routing options. In particular, we start by the shortest path for each OD pair. Then, we remove the edges in this path and go with the second shortest path, and we continue this process until we find 4 different routes between the origin and destination (or no other routes exist). We use the model in [64] to compute the probability of accepting different offers on the different routes for each individual driver. This model is based on a utility function that considers the travel time of the path, and the value of the offered incentive to predict the probability of its acceptance. Notice that this model is "personalized" since different individuals respond differently to the same incentive. In particular, features such as gender, salary, or level of education can influence the individual's response to the offered incentive [64]. Thus, this model includes individual features such as the salary and education of the drivers to model their behavior. In our numerical experiments,

however, due to lack of data about each individual's features, we only consider the travel time of the path and the value of the offered incentive. Moreover, in our experiments, we assume that we have access to all the drivers that are currently in the system and we can offer an incentive to each individual one. If we have access to a portion of drivers, we can simply consider a zero value of incentive in our utility function and compute the probability of different paths based on their total travel time.

Experiment I

In Experiment I, we check the performance of models (3) and (4) using the ADMS data for May, 5^{th} of 2018 with the incentive set $\mathcal{I} = \{\$0, \$1, \$2, \$5, \$10, \$1000\}$. The region considered in our analysis is depicted in Figure 1. This region includes the data of 301 sensors. Based on the ADMS data, we created a graph with 41 nodes and 139 links. OD points are located on intersections and close to the ramp of the highways. The number of OD pairs is 1681 and there are 4286 paths between them in total. The estimated total number of drivers incoming to the system between 5 AM to 9 AM by the OD estimation algorithm is depicted in Figure 2. Results of model (3) are presented in Table 1, Table 2, and Table 3; and the results of model (4) are presented in Tables 4, 5, and 6.

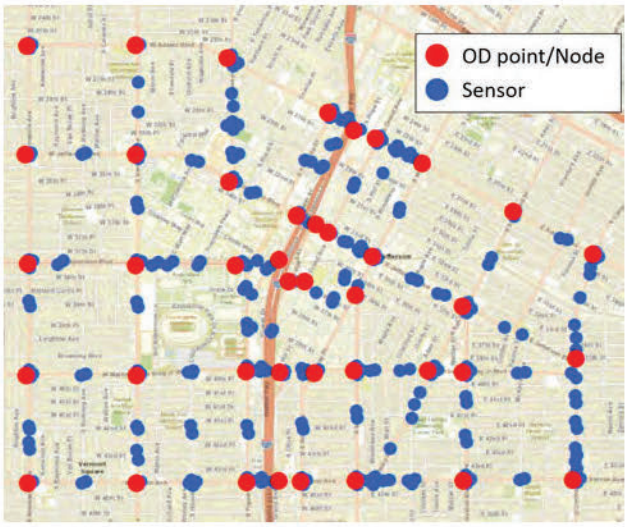

Figure 1. Region set

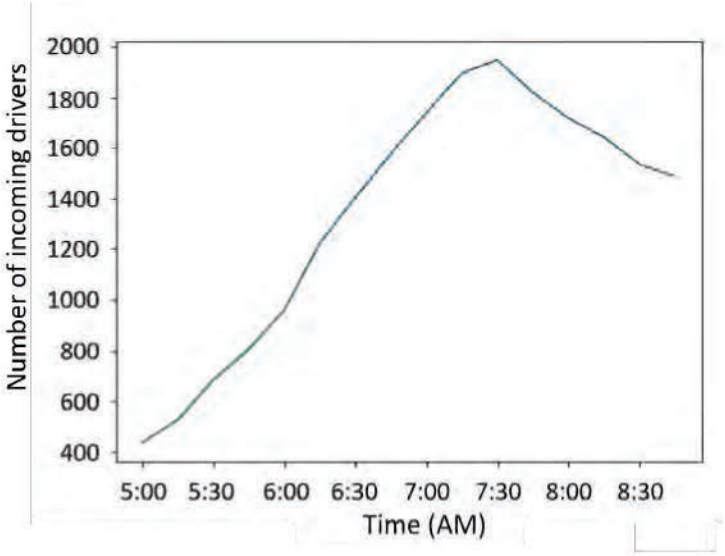

Figure 2. Total estimated number of drivers entering the system (in 15 minute intervals)

Notice that these models may result in infeasible optimization problems. Hence, we included a parameter α in our formulation as the multiplier of the allowed capacity. For instance, $\alpha = 2.0$ means that the optimization model tries to keep all traffic flows beyond twice the nominal capacity of the links. We only consider this multiplier during the computation of incentives; however, during the computation of Carbon emission and total travel time we use the original capacity. In this experiment, we use Google services to compute distances between various nodes, we also pick the route with highest probability for each driver when no incentive is offered (i.e., we assumed zero incentive in our probabilistic model for such drivers). To compute the Carbon emission, we need the expected total travel time based on the expected volume of the links after incentive assignments which is presented as total travel time in the tables below. The

"CO_2 decrease" column is the percentage of decrease of Carbon emission compared to the scenario where no incentive is provided.

Table 1. Experiment I for model (3), traffic of 6-7 AM

Time: 6-7 AM				
α parameter	Cost ($)	CO_2 ($g \times 10^6$)	CO_2 decrease	Total travel time (hour)
α = 1.5	Infeasible			
α = 2.0	306	2.874	0.24%	420.22

Table 2: Experiment I for model (3), traffic of 7-8 AM

Time: 7-8 AM				
α parameter	Cost ($)	CO_2 ($g \times 10^6$)	CO_2 decrease	Total travel time (hour)
α = 1.5	Infeasible			
α = 2.0	952	4.578	0.82%	720.18

Table 3: Experiment I for model (3), traffic of 8-9 AM

Time: 8-9 AM				
α parameter	Cost ($)	CO_2 ($g \times 10^6$)	CO_2 decrease	Total travel time (hour)
α = 1.0	Infeasible			
α = 1.5	4512	3.781	4.59%	538.18
α = 2.0	422	3.925	0.96%	593.11

As can be seen in Tables 1,2, and 3, the optimal choice of α is not clear before tuning and it requires a line search to identify it. Due to the high traffic volume between 6 AM and 9 AM (rush hours), traffic is beyond the capacity of the roads so with the original capacity of the road ($\alpha = 1.0$) or even higher capacity ($\alpha = 1.5$), we cannot satisfy the demand in all the road segments. Hence, in model (3), we need to find out the reasonable capacity (by tuning α) in which we do not have infeasibility.

Table 4: Experiment I for model (4), traffic of 6-7 AM

	Time: 6-7 AM				
	Budget ($\$ \times 10^3$)				
	0	0.1	1	10	100
Cost ($\$ \times 10^3$)	0	100	1	10	99.35
CO_2 ($g \times 10^6$)	2.881	2.863	2.741	2.366	2.311
CO_2 decrease	0%	0.62%	4.86%	17.88%	19.78%
Total travel time (hour)	431.37	428.97	410.01	365.36	371.37

Table 5: Experiment I for model (4), traffic of 7-8 AM

	Time: 7-8 AM				
	Budget ($\$ \times 10^3$)				
	0	0.1	1	10	100
Cost ($\$ \times 10^3$)	0	100	1	10	99.955
CO_2 ($g \times 10^6$)	4.616	4.593	4.416	3.795	3.659
CO_2 decrease	0%	0.5%	4.33%	17.79%	20.73%
Total travel time (hour)	769.32	764.55	721.66	615.78	633.13

Table 6: Experiment I for model (4), traffic of 8-9 AM

	Time: 8-9 AM				
	Budget ($\$ \times 10^3$)				
	0	0.1	1	10	100
Cost ($\$ \times 10^3$)	0	100	1	10	99.138
CO_2 ($g \times 10^6$)	3.963	3.939	3.783	3.222	3.134

CO_2 decrease	0%	0.61%	4.54%	18.70%	20.92%
Total travel time (hour)	615.60	610.86	582.12	492.95	507.13

As can be seen in the above tables, when the available budget increases, the central planner can reduce congestion further, which in turn results in lower CO_2 emissions and a decreased total travel time. Moreover, we observe that there is a diminishing return when we increase the budget. For example, in Table 5 and Table 6, when the budget is increased from \$1000 to \$10,000, the CO_2 emission decrease is improved by almost a factor of 4. However, increasing the budget further to \$100,000 will only slightly improve the total CO_2 emissions of the system.

Experiment II

In Experiment II, we evaluate the performance of our methods in a slightly different setting. In this setting, the incentive set is $\{\$0, \$2, \$10\}$. The region under analysis is similar to the region in Experiment I, which is depicted in Figure 2. But in this region, we decreased the number of OD points to 17 to shrink the size of the data. The number of OD pairs becomes 289 and there are 672 paths between them in total. The estimated total number of drivers incoming to the system between 5 AM to 9 AM by the OD estimation algorithm is depicted in Figure 4.

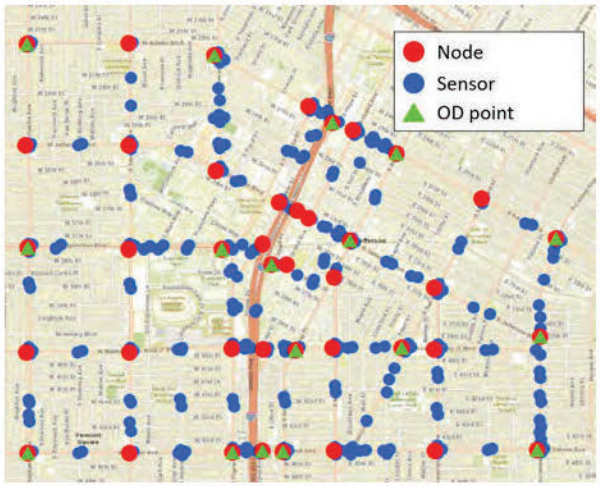

Figure 3. Region set II.

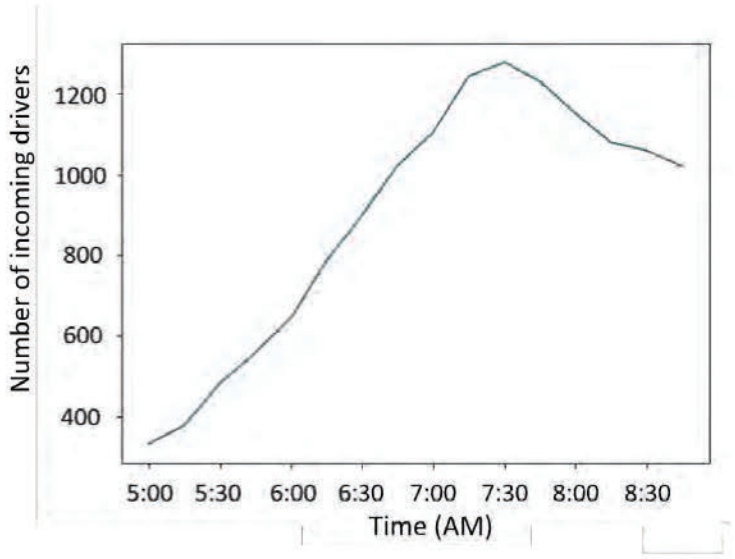

Figure 4. Total estimated number of drivers entering the system (in 15 minute intervals).

Table 7: Experiment II for model (3), traffic of 6-7 AM

Time: 6-7 AM				
α parameter	Cost ($)	CO_2 ($g \times 10^6$)	CO_2 decrease	Total travel time (hour)
$\alpha = 2.0$	Infeasible			

Table 8: Experiment II for model (3), traffic of 7-8 AM

Time: 7-8 AM				
α parameter	Cost ($)	CO_2 ($g \times 10^6$)	CO_2 decrease	Total travel time (hour)
$\alpha = 2.0$	Infeasible			

Table 9: Experiment II for model (3), traffic of 8-9 AM

Time: 8-9 AM				
α parameter	Cost ($)	CO_2 ($g \times 10^6$)	CO_2 decrease	Total travel time (hour)
$\alpha = 2.0$	Infeasible			

Table 10: Experiment II for model (4), traffic of 6-7 AM

	Time: 6-7 AM				
	Budget ($\$ \times 10^3$)				
	0	0.1	1	10	100
Cost ($\$ \times 10^3$)	0	100	1	10	31.428
CO_2 ($g \times 10^6$)	2.544	2.524	2.429	2.242	2.242
CO_2 decrease	0%	0.79%	4.52%	11.87%	11.87%
Total travel time (hour)	386.39	383.47	375.39	433.09	513.99

Table 11: Experiment II for model (4), traffic of 7-8 AM

	Time: 7-8 AM				
	Budget ($\$ \times 10^3$)				
	0	0.1	1	10	100
Cost ($\$ \times 10^3$)	0	100	1	10	44.536
CO_2 ($g \times 10^6$)	4.073	4.054	3.921	3.729	3.818
CO_2 decrease	0%	0.47%	3.73%	8.45%	6.26%
Total travel time (hour)	707.38	704.69	681.99	967.51	1281.26

Table 12: Experiment II for model (4), traffic of 8-9 AM

	Time: 8-9 AM				
	Budget ($\$ \times 10^3$)				
	0	0.1	1	10	100
Cost ($\$ \times 10^3$)	0	100	1	10	39.302
CO_2 ($g \times 10^6$)	3.562	3.540	3.415	3.199	3.272

CO_2 decrease	0%	0.62%	4.13%	10.19%	8.14%
Total travel time (hour)	561.21	557.73	535.15	665.68	935.47

Again, we observe that increasing the budget will result in lower traffic volumes, lower CO_2 emissions, and shorter total travel time. We also observe the diminishing return phenomenon when increasing the budget, as described before.

Experiment III

In Experiment III, we evaluate the performance of our methods in a similar setting as Experiment I but for a different region. This region includes the highways of a portion of Los Angeles county depicted in Figure 5.. There are 25 OD points in this region with 625 OD pairs, resulting in 1331 paths between them in total. The estimated number of drivers entering the system between 5 AM to 9 AM is depicted in Figure 6.

Figure 5. Studied region for experiment III

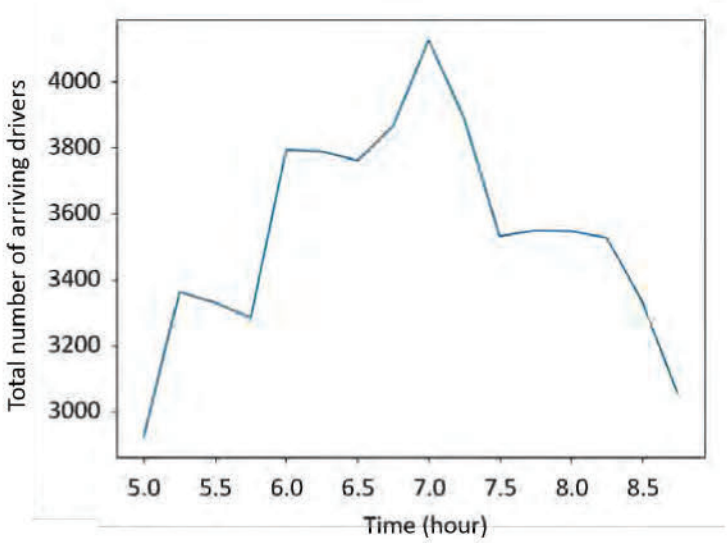

Figure 6. Estimated number of drivers entering the system

Table 13: Experiment III for model (3), traffic of 6-7 AM

Time: 6-7 AM				
α parameter	Cost ($)	CO_2 (g $\times 10^6$)	CO_2 decrease	Total travel time (hour)
$\alpha = 1.0$	Infeasible			
$\alpha = 1.5$	6866	57.390	3.73%	4324.12
$\alpha = 2.0$	2591	58.355	2.11%	4449.03

Table 14: Experiment III for model (3), traffic of 7-8 AM

Time: 7-8 AM				
α parameter	Cost ($)	CO_2 (g $\times 10^6$)	CO_2 decrease	Total travel time (hour)
$\alpha = 1.0$	Infeasible			
$\alpha = 1.5$	5450	53.748	4.07%	3932.50
$\alpha = 2.0$	2308	54.508	2.71%	4035.53

Table 15: Experiment III for model (3), traffic of 8-9 AM

Time: 8-9 AM				
α parameter	Cost ($)	CO_2 ($g \times 10^6$)	CO_2 decrease	Total travel time (hour)
$\alpha = 1.0$	Infeasible			
$\alpha = 1.5$	3936	48.64	4.04%	3406.33
$\alpha = 2.0$	1715	49.387	2.56%	3527.92

Table 16: Experiment III for model (4), traffic of 6-7 AM

	Time: 6-7 AM				
	Budget ($\$ \times 10^3$)				
	0	0.1	1	10	100
Cost ($\$ \times 10^3$)	0	100	1	10	99.11
CO_2 ($g \times 10^6$)	59.615	59.567	59.366	56.928	56.087
CO_2 decrease	0%	0.08%	0.42%	4.51%	5.92%
Total travel time (hour)	5412.54	5403.76	5376.96	4640.98	5009.11

Table 17: Experiment III for model (4), traffic of 7-8 AM

	Time: 7-8 AM				
	Budget ($\$ \times 10^3$)				
	0	0.1	1	10	100
Cost ($\$ \times 10^3$)	0	100	1	10	99.33
CO_2 ($g \times 10^6$)	56.028	55.982	55.625	52.836	51.738
CO_2 decrease	0%	0.08%	0.72%	5.70%	7.66%

Total travel time (hour)	4834.51	4817.06	4737.40	4078.53	4737.25

Table 18: Experiment III for model (4), traffic of 8-9 AM

	Time: 8-9 AM				
	Budget ($\$ \times 10^3$)				
	0	0.1	1	10	100
Cost ($\$ \times 10^3$)	0	100	1	10	99.681
CO_2 ($g \times 10^6$)	50.686	50.65	50.276	47.533	46.105
CO_2 decrease	0%	0.07%	0.81%	6.22%	9.04%
Total travel time (hour)	4087.44	4078.89	4019.53	3482.51	4172.35

Experiment IV

In Experiment IV, we evaluate the performance of our methods in a similar setting as Experiment II with the region being similar to the region in Experiment III.

Table 19: Experiment III for model (3), traffic of 6-7 AM

Time: 6-7 AM				
α parameter	Cost ($)	CO_2 ($g \times 10^6$)	CO_2 decrease	Total travel time (hour)
$\alpha = 1.0$	Infeasible			
$\alpha = 1.5$	6866	57.390	3.73%	4324.12
$\alpha = 2.0$	2591	58.355	2.11%	4449.03

Table 20: Experiment III for model (3), traffic of 7-8 AM

Time: 7-8 AM				
α parameter	Cost ($)	CO_2 ($g \times 10^6$)	CO_2 decrease	Total travel time (hour)
$\alpha = 1.0$	Infeasible			

α = 1.5	5450	53.748	4.07%	3932.50
α = 2.0	2308	54.508	2.71%	4035.53

Table 21: Experiment III for model (3), traffic of 8-9 AM

Time: 8-9 AM				
α parameter	Cost ($)	CO_2 ($g \times 10^6$)	CO_2 decrease	Total travel time (hour)
α = 1.0	Infeasible			
α = 1.5	3936	48.64	4.04%	3406.33
α = 2.0	1715	49.387	2.56%	3527.92

Table 22: Experiment III for model (4), traffic of 6-7 AM

	Time: 6-7 AM				
	Budget ($\$ \times 10^3$)				
	0	0.1	1	10	100
Cost ($\$ \times 10^3$)	0	100	1	10	99.11
CO_2 ($g \times 10^6$)	59.615	59.567	59.366	56.928	56.087
CO_2 decrease	0%	0.08%	0.42%	4.51%	5.92%
Total travel time (hour)	5412.54	5403.76	5376.96	4640.98	5009.11

Table 23: Experiment III for model (4), traffic of 7-8 AM

	Time: 7-8 AM				
	Budget ($\$ \times 10^3$)				
	0	0.1	1	10	100
Cost ($\$ \times 10^3$)	0	100	1	10	99.33
CO_2 ($g \times 10^6$)	56.028	55.982	55.625	52.836	51.738

CO_2 decrease	0%	0.08%	0.72%	5.70%	7.66%
Total travel time (hour)	4834.51	4817.06	4737.40	4078.53	4737.25

Table 24: Experiment III for model (4), traffic of 8-9 AM

	Time: 8-9 AM				
	Budget ($\$ \times 10^3$)				
	0	0.1	1	10	100
Cost ($\$ \times 10^3$)	0	100	1	10	99.681
CO_2 ($g \times 10^6$)	50.686	50.65	50.276	47.533	46.105
CO_2 decrease	0%	0.07%	0.81%	6.22%	9.04%
Total travel time (hour)	4087.44	4078.89	4019.53	3482.51	4172.35

Table 25 summarizes the result of experiments I and II and Table 26 summarizes the result of experiments III and IV for 7-9 AM (which can be considered as rush hour times in Los Angeles). We observe that increasing the budget results in higher average amount of offered incentives, higher percentage of drivers to whom we offered the incentive, and higher reduction in Carbon emissions. The improvement in the reduction of Carbon emissions is by a factor of almost 4 and 2 in experiments I and II respectively when the budget is increased. Also, the improvement in the reduction of Carbon emissions is by a factor of almost 8 in experiments III and IV when the budget is increased. For more details about the distribution of offered incentives to the drivers at 7-8 AM and 8-9 AM in experiments I , II, III, and IV please see Table 28-Table 35 in the appendix section.

Table 25: Comparison of $1k and $10k budget for 7-8 AM and 8-9 AM in experiment I and II.

	Number of drivers entering the system	Budget ($\$ \times 10^3$)	Percentage of drivers to whom we offered incentive	Average of the incentive amount	Reduction in Carbon Emission
7-8 AM Exp. I	7402	1	8.94%	1.51	4.33%
		10	43.12%	3.13	17.79%
8-9 AM Exp. I	6380	1	9.86%	1.59	4.54%
		10	47.46%	3.30	18.70%
7-8 AM Exp. II	4856	1	10.30%	2	3.73%
		10	79.08%	2.60	8.45%
8-9 AM Exp. II	4308	1	11.61%	2	4.13%
		10	79.67%	2.91	10.19%

In addition, Table 25 shows that even offering incentives to 9% of the vehicles (with the average of $1.5 monetary incentive per driver) can reduce the CO_2 emissions by 4%. If approximately 45% of the drivers are incentivized with the average of $2-$3 per driver, the CO_2 emissions can reduce by more than 20%. Moreover, we observe a *diversity gain* in Experiment I compared to Experiment II. More precisely, in Experiment I where the number of possible ODs is larger, we obtain further improvement in congestion reduction by increasing the monetary budget.

Table 26: Comparison of $1k and $10k budget for 7-8 AM and 8-9 AM in experiment I and II.

	Number of drivers entering the system	Budget ($\$ \times 10^3$)	Percentage of drivers to whom we offered incentive	Average of the incentive amount	Reduction in Carbon Emission
7-8 AM Exp. III	15096	1	3.78%	1.75	0.72%
		10	21.91%	3.02	5.70%
8-9 AM Exp. III	13463	1	2.91%	2.55	0.81%
		10	23.35%	3.18	6.22%
7-8 AM Exp. IV	15096	1	2.99%	2.21	0.69%
		10	21.30%	3.11	5.33%
8-9 AM Exp. IV	13463	1	2.93%	2.53	0.46%
		10	21.15%	3.51	5.56%

Table 26 shows that offering incentives to 1.75% of the vehicles in the large portion of Los Angeles county (with the average of $1.75 monetary incentive per driver) can reduce the CO_2 emissions by 0.72%. If approximately 21.91% of the drivers are incentivized with the average of $3 per driver, the CO_2 emissions can reduce by more than 5%. Although the percentage of reduction in Experiment III and IV is smaller than Experiment I and II, we should consider that Experiment III and IV includes much larger area than Experiment I and II and the scale of Carbon reduction is different. Furthermore, we observe a *diversity gain* in Experiment III compared to Experiment IV which was observed in Experiment III and IV as well. For more details about the distribution of offered incentives to drivers at 7-8 AM and 8-9 AM in experiment I, please see Table 28 to Table 35in the appendix.

Conclusion

In this project, we developed mathematical models and proposed algorithms for offering personalized incentives to drivers to reduce congestion in the network. In this framework, drivers share their origin-destination and routing information with a central planner. Based on this information, the central planner then offers incentives to drivers to incentivize/enforce a socially

optimal routing strategy. The incentives are offered based on solving a large-scale optimization problem in our framework. In our framework, we bring together prior works to model the behavior of drivers in response to the offered incentives as well as the resulting congestion reduction in the network. We consider different formulations such as optimizing a utility of traffic flows subject to budget constraints; or minimizing the cost of offering incentives subject to traffic flow constraints. We also pay special attention to minimizing the carbon emission of the network and show that this problem leads to a convex optimization problem in our data. In addition, we showed that this problem can be solved in a distributed fashion where some of the computations are performed on individual drivers' smart devices. Finally, we evaluated the performance of some of our models and algorithms using the Archived Data Management System (ADMS) data. Our experiments show that the proposed framework can lead up to a 27% decrease in the total carbon emission of the system during rush hour times.

In this work, the incentives are only offered to alter the routing decision of the drivers. As future work, it is crucial to look at the effect of offering incentives to change the mode or time of the drivers' trips. These options will bring additional flexibility to the model, which in turn will result in further congestion reduction.

References

[1] Michael J. Sprung, Matthew Chambers, and Sonya Smith-Pickel. chapter Transportation Statistics Annual Report 2018. Dec 2018. Tech Report.

[2] INRIX 2018 global traffic scorecard. https://inrix.com/scorecard/. Accessed: 2020-01-19.

[3] INRIX 2019 Los Angeles traffic scorecard. https://inrix.com/scorecard-city/?city=Los%20Angeles%2C%20CA&index=26. Accessed: 2021-02-16.

[4] Congestion mitigation and air quality improvement program: Assessing 10 years of experience. http://www.trb.org/main/blurbs/160904.aspx.

[5] Health Effects Institute. Panel on the Health Effects of Traffic-Related Air Pollution. Traffic-related air pollution: a critical review of the literature on emissions, exposure, and health effects. Number 17. Health Effects Institute, 2010.

[6] Kai Zhang and Stuart Batterman. Air pollution and health risks due to vehicle traffic. Science of the total Environment, 450:307–316, 2013.

[7] Dwight A Hennessy and David L Wiesenthal. Traffic congestion, driver stress, and driver aggression. Aggressive Behavior: Official Journal of the International Society for Research on Aggression, 25(6):409–423, 1999.

[8] Melvin L Selzer and Amiram Vinokur. Life events, subjective stress, and traffic accidents. American Journal of Psychiatry, 131(8):903–906, 1974.

[9] Cambridge Systematics. Traffic congestion and reliability: Trends and advanced strategies for congestion mitigation. Technical report, United States. Federal Highway Administration, 2005.

[10] Robert Cervero. Road expansion, urban growth, and induced travel: A path analysis. Journal of the American Planning Association, 69(2):145–163, 2003.

[11] Jonathan Vespa, David M Armstrong, and Lauren Medina. Demographic turning points for the United States: Population projections for 2020 to 2060. US Department of Commerce, Economics and Statistics Administration, 2018.

[12] Arthur C Pigou. The economics of welfare Macmillan and Co. London, United Kingdom, 1920.

[13] Frank H Knight. Some fallacies in the interpretation of social cost. The Quarterly Journal of Economics, 38(4):582–606, 1924.

[14] Erik Verhoef, Michiel C.J. Bliemer, Linda Steg, and Bert van Wee, editors. Pricing in Road Transport. Number 4192 in Books. Edward Elgar Publishing, July 2008.

[15] Dirk Hendrik Van Amelsfort. Behavioural responses and network effects of time-varying road pricing. 2009.

[16] Nan Zheng, Guillaume Rérat, and Nikolas Geroliminis. Time-dependent area-based pricing for multi- modal systems with heterogeneous users in an agent-based environment. Transportation Research Part C: Emerging Technologies, 62:133–148, 2016.

[17] Carlos F Daganzo and Lewis J Lehe. Distance-dependent congestion pricing for downtown zones. Transportation Research Part B: Methodological, 75:89–99, 2015.

[18] Shu Zhang, Ann M Campbell, and Jan F Ehmke. Impact of congestion pricing schemes on costs and emissions of commercial fleets in urban areas. Networks, 73(4):466–489, 2019.

[19] Jasper Knockaert, Yin-Yen Tseng, Erik T Verhoef, and Jan Rouwendal. The Spitsmijden experiment: A reward to battle congestion. Transport Policy, 24:260–272, 2012.

[20] David Levinson. Equity effects of road pricing: A review. Transport Reviews, 30(1):33–57, 2010.

[21] Karel Martens, Aaron Golub, and Glenn Robinson. A justice-theoretic approach to the distribution of transportation benefits: Implications for transportation planning practice in the united states. Transportation Research Part A: Policy and Practice, 46(4):684–695, 2012.

[22] Bernhard Schlag and Ulf Teubel. Public acceptability of transport pricing. IATSS research, 21:134–142, 1997.

[23] Charles Raux and Stéphanie Souche. The acceptability of urban road pricing: A theoretical analysis applied to experience in lyon. Journal of Transport Economics and Policy (JTEP), 38(2):191–215, 2004.

[24] Petros Ieromonachou, Stephen Potter, and James P Warren. Evaluation of the implementation process of urban road pricing schemes in the United Kingdom and Italy. European Transport, 32:49–68, 2006.

[25] Ziyuan Gu, Zhiyuan Liu, Qixiu Cheng, and Meead Saberi. Congestion pricing practices and public acceptance: A review of evidence. Case Studies on Transport Policy, 6(1):94–101, 2018.

[26] Ziyuan Gu, Sajjad Shafiei, Zhiyuan Liu, and Meead Saberi. Optimal distance-and time-dependent area-based pricing with the network fundamental diagram. Transportation Research Part C: Emerging Technologies, 95:1–28, 2018.

[27] Erik Verhoef, Peter Nijkamp, and Piet Rietveld. Tradeable permits: their potential in the regulation of road transport externalities. Environment and Planning B: Planning and Design, 24(4):527–548, 1997.

[28] Jose M Viegas. Making urban road pricing acceptable and effective: searching for quality and equity in urban mobility. Transport Policy, 8(4):289–294, 2001.

[29] Charles Raux. The use of transferable permits in transport policy. Transportation Research Part D: Transport and Environment, 9(3):185–197, 2004.

[30] Wenbo Fan and Xinguo Jiang. Tradable mobility permits in roadway capacity allocation: Review and appraisal. Transport Policy, 30:132–142, 2013.

[31] John Thøgersen and Berit Møller. Breaking car use habits: The effectiveness of a free one-month travelcard. Transportation, 35(3):329–345, 2008.

[32] Guangmin Wang, Ziyou Gao, Meng Xu, and Huijun Sun. Models and a relaxation algorithm for continuous network design problem with a tradable credit scheme and equity constraints. Computers & Operations Research, 41:252–261, 2014.

[33] Theodore Tsekeris and Stefan Voß. Design and evaluation of road pricing: state-of-the-art and methodological advances. NETNOMICS: Economic Research and Electronic Networking, 10(1):5–52, 2009.

[34] Yu Marco Nie. A new tradable credit scheme for the morning commute problem. Networks and Spatial Economics, 15(3):719–741, 2015.

[35] Di Wu, Yafeng Yin, Siriphong Lawphongpanich, and Hai Yang. Design of more equitable congestion pricing and tradable credit schemes for multimodal transportation networks. Transportation Research Part B: Methodological, 46(9):1273–1287, 2012.

[36] Susan Grant-Muller and Meng Xu. The role of tradable credit schemes in road traffic congestion management. Transport Reviews, 34(2):128–149, 2014.

[37] Hideki Fukui. An empirical analysis of airport slot trading in the United States. Transportation Research Part B: Methodological, 44(3):330–357, 2010.

[38] Nico Dogterom, Dick Ettema, and Martin Dijst. Tradable credits for managing car travel: a review of empirical research and relevant behavioural approaches. Transport Reviews, 37(3):322–343, 2017.

[39] Carlos Lima Azevedo, Ravi Seshadri, Song Gao, Bilge Atasoy, Arun Prakash Akkinepally, Eleni Christofa, Fang Zhao, Jessika Trancik, and Moshe Ben-Akiva. Tripod: sustainable travel incentives with prediction, optimization, and personalization. In Transportation Research Board 97th Annual Meeting, 2018.

[40] Jack Williams Brehm. A Theory of Psychological Reactance. New York: Academic Press, 1966.

[41] J Knockaert, M Bliemer, D Ettema, D Joksimovic, A Mulder, J Rouwendal, and D Van Amelsfort. Experimental design and modelling Spitsmijden. Utrecht, Consortium Spitsmijden, 2007.

[42] David M Kreps. Intrinsic motivation and extrinsic incentives. The American Economic Review, 87(2):359–364, 1997.

[43] Kent C Berridge. Reward learning: Reinforcement, incentives, and expectations. In Psychology of Learning and Motivation, volume 40, pages 223–278. Elsevier, 2000.

[44] Deepak Merugu, Balaji S Prabhakar, and N Rama. An incentive mechanism for decongesting the roads: A pilot program in Bangalore. In Proc. of ACM NetEcon Workshop. Citeseer, 2009.

[45] Jia Shuo Yue, Chinmoy V Mandayam, Deepak Merugu, Hossein Karkeh Abadi, and Balaji Prabhakar. Reducing road congestion through incentives: a case study. 2015.

[46] Michiel Bliemer, Matthijs Dicke-Ogenia, and Dick Ettema. Rewarding for avoiding the peak period: A synthesis of three studies in the Netherlands. In European Transport Conference 2009. Citeseer, 2009.

[47] Eran Ben-Elia, Dick Ettema, and Hennie Boeije. Behaviour change dynamics in response to rewarding rush-hour avoidance: A qualitative research approach. 2011.

[48] Eran Ben-Elia and Dick Ettema. Changing commuters' behavior using rewards: A study of rush-hour avoidance. Transportation research part F: Traffic Psychology and Behaviour, 14(5):354–368, 2011.

[49] Xianbiao Hu, Yi-Chang Chiu, and Lei Zhu. Behavior insights for an incentive-based active demand management platform. International Journal of Transportation Science and Technology, 4(2):119–133, 2015.

[50] Vivek Kumar, Chandra R Bhat, Ram M Pendyala, Daehyun You, Eran Ben-Elia, and Dick Ettema. Impacts of incentive-based intervention on peak period traffic: experience from the Netherlands. Transportation Research Record, 2543(1):166–175, 2016.

[51] Satoshi Fuji and Ryuichi Kitamura. What does a one-month free bus ticket do to habitual drivers. Transportation, 30:81–95, 2003.

[52] Sebastian Bamberg, Icek Ajzen, and Peter Schmidt. Choice of travel mode in the theory of planned behavior: The roles of past behavior, habit, and reasoned action. Basic and Applied Social Psychology, 25(3):175–187, 2003.

[53] Graham Currie. Free fare incentives to shift rail demand peaks–medium-term impacts. Technical report, 2011.

[54] Zheng Zhang, Hidemichi Fujii, and Shunsuke Managi. How does commuting behavior change due to incentives? an empirical study of the Beijing subway system. Transportation Research Part F: Traffic Psychology and Behaviour, 24:17–26, 2014.

[55] Shiwali Mohan, Matthew Klenk, and Victoria Bellotti. Exploring how to personalize travel mode recommendations for urban transportation. In IUI Workshops, 2019.

[56] Xi Zhu, Feilong Wang, Cynthia Chen, and Derek D Reed. Personalized incentives for promoting sustainable travel behaviors. Transportation Research Part C: Emerging Technologies, 2019.

[57] Yaguang Li, Rose Yu, Cyrus Shahabi, and Yan Liu. Diffusion convolutional recurrent neural network: Data-driven traffic forecasting. In International Conference on Learning Representations, 2018.

[58] Ting Yu, Haoteng Yin, and Zhanxing Zhu. Spatio-temporal graph convolutional networks: A deeplearning framework for traffic forecasting. In IJCAI, 2018.

[59] Emilian Necula. Dynamic traffic flow prediction based on GPS data. In 2014 IEEE 26th International Conference on Tools with Artificial Intelligence, pages 922–929. IEEE, 2014.

[60] Huaxiu Yao, Xianfeng Tang, Hua Wei, Guanjie Zheng, and Zhenhui Li. Revisiting spatial-temporal similarity: A deep learning framework for traffic prediction. In Proceedings of the AAAI Conference on Artificial Intelligence, volume 33, pages 5668–5675, 2019.

[61] Xiaolei Ma, Zhuang Dai, Zhengbing He, Jihui Ma, Yong Wang, and Yunpeng Wang. Learning traffic as images: a deep convolutional neural network for large-scale transportation network speed prediction. Sensors, 17(4):818, 2017.

[62] Zhiyong Cui, Kristian Henrickson, Ruimin Ke, and Yinhai Wang. Traffic graph convolutional recurrent neural network: A deep learning framework for network-scale traffic learning and forecasting. IEEE Transactions on Intelligent Transportation Systems, volume 21, Issue 11, pages 4883–4894, 2020.

[63] Robust traffic prediction. https://github.com/optimization-for-data-driven-science/Reliable-Traffic-Prediction.

[64] Chenfeng Xiong, Mehrdad Shahabi, Jun Zhao, Yafeng Yin, Xuesong Zhou, and Lei Zhang. An integrated and personalized traveler information and incentive scheme for energy efficient mobility systems. Transportation Research Part C: Emerging Technologies, volume 113, pages 57–73, 2020.

[65] Wei Ma and Zhen Sean Qian. Estimating multi-year 24/7 origin-destination demand using high-granular multi-source traffic data. Transportation Research Part C: Emerging Technologies, 96:96–121, 2018.

[66] PG Boulter and IS McCrae. Artemis: Assessment and reliability of transport emission models and inventory systems-final report. TRL Published Project Report, 2007.

[67] R Pachauri and L Meyer. Climate change 2014: Synthesis report. fifth assessment report of the intergovernmental panel on climate change. Tech. Rep., 2014.

[68] United States. Bureau of Public Roads. Traffic assignment manual for application with a large, high speed computer, volume 37. US Department of Commerce, Bureau of Public Roads, Office of Planning, Urban Planning Division, 1964.

[69] Michael Grant and Stephen Boyd. CVX: Matlab software for disciplined convex programming, version 2.1. http://cvxr.com/cvx, March 2014.

[70] Michael Grant and Stephen Boyd. Graph implementations for nonsmooth convex programs. In V. Blondel, S. Boyd, and H. Kimura, editors, Recent Advances in Learning and Control, Lecture Notes in Control and Information Sciences, pages 95–110. Springer-Verlag Limited, 2008. http://stanford.edu/~boyd/graph_dcp.html.

[71] Stephen Boyd, Neal Parikh, and Eric Chu. Distributed optimization and statistical learning via the alternating direction method of multipliers. Now Publishers Inc, 2011.

[72] Daniel Gabay and Bertrand Mercier. A dual algorithm for the solution of nonlinear variational problems via finite element approximation. Computers & Mathematics with Applications, 2(1):17–40, 1976.

[73] Roland Glowinski and A Marroco. Sur l'approximation, par éléments finis d'ordre un, et la résolution, par pénalisation-dualité d'une classe de problèmes de dirichlet non linéaires. ESAIM: Mathematical Modelling and Numerical Analysis-Modélisation Mathématique et Analyse Numérique, 9(R2):41–76, 1975.

[74] Mingyi Hong, Zhi-Quan Luo, and Meisam Razaviyayn. Convergence analysis of alternating direction method of multipliers for a family of nonconvex problems. SIAM Journal on Optimization, 26(1):337– 364, 2016.

[75] Shaokai Ye, Tianyun Zhang, Kaiqi Zhang, Jiayu Li, Kaidi Xu, Yunfei Yang, Fuxun Yu, Jian Tang, Makan Fardad, Sijia Liu, et al. Progressive weight pruning of deep neural networks using ADMM. arXiv preprint arXiv:1810.07378, 2018.

[76] Shaokai Ye, Xiaoyu Feng, Tianyun Zhang, Xiaolong Ma, Sheng Lin, Zhengang Li, Kaidi Xu, Wujie Wen, Sijia Liu, Jian Tang, et al. Progressive DNN compression: A key to achieve ultra-high weight pruning and quantization rates using ADMM. arXiv preprint arXiv:1903.09769, 2019.

[77] Yong Yuan, Chen Chen, Xiyuan Hu, and Silong Peng. TP-ADMM: An efficient two-stage framework for training binary neural networks. In International Conference on Neural Information Processing, pages 580–588. Springer, 2019.

[78] Geng Yuan, Xiaolong Ma, Caiwen Ding, Sheng Lin, Tianyun Zhang, Zeinab S Jalali, Yilong Zhao, Li Jiang, Sucheta Soundarajan, and Yanzhi Wang. An ultra-efficient memristor-based DNN framework with structured weight pruning and quantization using ADMM. In 2019 IEEE/ACM International Symposium on Low Power Electronics and Design (ISLPED), pages 1–6. IEEE, 2019.

[79] Cong Leng, Zesheng Dou, Hao Li, Shenghuo Zhu, and Rong Jin. Extremely low bit neural network: Squeeze the last bit out with ADMM. In Thirty-Second AAAI Conference on Artificial Intelligence, 2018.

[80] Sheng Lin, Xiaolong Ma, Shaokai Ye, Geng Yuan, Kaisheng Ma, and Yanzhi Wang. Toward extremely low bit and lossless accuracy in DNNs with progressive ADMM. arXiv preprint arXiv:1905.00789, 2019.

[81] Tianyun Zhang, Shaokai Ye, Kaiqi Zhang, Jian Tang, Wujie Wen, Makan Fardad, and Yanzhi Wang. A systematic DNN weight pruning framework using alternating direction method of multipliers. In Proceedings of the European Conference on Computer Vision (ECCV), pages 184–199, 2018.

[82] Ning Liu, Xiaolong Ma, Zhiyuan Xu, Yanzhi Wang, Jian Tang, and Jieping Ye. Autocompress: An automatic DNN structured pruning framework for ultra-high compression rates. In AAAI, pages 4876–4883, 2020.

[83] Ao Ren, Tianyun Zhang, Shaokai Ye, Jiayu Li, Wenyao Xu, Xuehai Qian, Xue Lin, and Yanzhi Wang. ADMM-NN: An algorithm-hardware co-design framework of DNNs using alternating direction methods of multipliers. In Proceedings of the Twenty-Fourth International Conference on Architectural Support for Programming Languages and Operating Systems, pages 925–938, 2019.

[84] Hongjia Li, Ning Liu, Xiaolong Ma, Sheng Lin, Shaokai Ye, Tianyun Zhang, Xue Lin, Wenyao Xu, and Yanzhi Wang. ADMM-based weight pruning for real-time deep learning acceleration on mobile devices. In Proceedings of the 2019 on Great Lakes Symposium on VLSI, pages 501–506, 2019.

[85] Tianjian Huang, Prajwal Singhania, Maziar Sanjabi, Pabitra Mitra, and Meisam Razaviyayn. Alternating direction method of multipliers for quantization. arXiv preprint arXiv:2009.03482, 2020.

[86] Henk J Van Zuylen and Luis G Willumsen. The most likely trip matrix estimated from traffic counts. Transportation Research Part B: Methodological, 14(3):281–293, 1980.

[87] Ennio Cascetta. Estimation of trip matrices from traffic counts and survey data: a generalized least squares estimator. Transportation Research Part B: Methodological, 18(4-5):289–299, 1984.

[88] Michael GH Bell. The real time estimation of origin-destination flows in the presence of platoon dispersion. Transportation Research Part B: Methodological, 25(2-3):115–125, 1991.

[89] Sharminda Bera and KV Rao. Estimation of origin-destination matrix from traffic counts: the state of the art. European Transport Trasporti Europei, 2011.

[90] Panchamy Krishnakumari, Hans van Lint, Tamara Djukic, and Oded Cats. A data driven method for od matrix estimation. Transportation Research Part C: Emerging Technologies, 2019.

[91] Stefano Carrese, Ernesto Cipriani, Livia Mannini, and Marialisa Nigro. Dynamic demand estimation and prediction for traffic urban networks adopting new data sources. Transportation Research Part C: Emerging Technologies, 81:83–98, 2017.

[92] Marialisa Nigro, Ernesto Cipriani, and Andrea del Giudice. Exploiting floating car data for time- dependent origin–destination matrices estimation. Journal of Intelligent Transportation Systems, 22(2):159–174, 2018.

[93] JinYoung Kim, Fumitaka Kurauchi, Nobuhiro Uno, Takeshi Hagihara, and Takehiko Daito. Using electronic toll collection data to understand traffic demand. Journal of Intelligent Transportation Systems, 18(2):190–203, 2014.

[94] Robert B Noland and Lewison L Lem. A review of the evidence forinduced travel and changes in transportation and environmental policy in the US and the UK. Transportation Research Part D: Transport and Environment, 7(1): 1–26, 2002.

[95] Susan Handy and Marlon G Boarnet. Impact of highway capacity and induced travel on passenger vehicle use and greenhouse gas emissions. California Environmental Protection Agency, Air Resources Board, Retrieved August, 28: 2015, 2014.

Data Management

Products of Research

Research products of this work will be submitted in peer-reviewed journal articles, book chapters and/or conference proceedings targeted towards the transportation science research community. All the resulting code for offering incentives are shared with Caltrans and NCST through DRYAD platform (DOI https://doi.org/10.5061/dryad.ncjsxkst8). In addition, the codes will be shared on the PI's repository (https://github.com/optimization-for-data-driven-science). Our goal is to make the use of our algorithm and its implementation convenient to the transportation science research community. The data format and the content of files shared on DRYAD is described next.

Data Format and Content

First, we imported the raw data from the ADMS system. Next, we preprocessed the data based on our criteria such the type of sensors, time interval of data, and region. Also, we extract the graph of the network on Networkx. Finally, we use the data for OD estimation and to solve our optimization model.

Our codes are in Python 2 and 3. Nine Python files have been produced in this project:

1. All_in_one1.py: This file generates two sets of files. It gets the preprocessed speed and volume data in CSV format and its output is pickled Pandas DataFrame format of both preprocessed data sets in separated files. Also, it gets the location data of sensors and computes the distance of sensors. Next, it creates the graph network by Networkx package and saves the file in pickled format. All the processes are in Python3 format. Running this code needs API key for Google Maps because we use Google service to find the distances.
2. All_in_one2.py: Inputs and outputs are same as All_in_one1.py but in Python2 format.
3. base.py: It includes functions that are used as tools in other Python files. For example, Path class is defined in this file.
4. data_loader.py: It consists of functions related to loading and saving data and their format.
5. address.py: It includes functions that create the address of output files.
6. link_capacity.py: This file generates the free flow travel time, free flow speed, and the capacity of links based on the BPR function by using Gradient Descent Method from PyTorch package. It also generates a CSV file including the distance of links with their ID. The input files are the speed data, volume data, and the graph of the network. This code is compatible with Python 3.
7. OptModel_linear1.py: The inputs are a YAML configuration file, graph of the network, free flow speed of links, capacity of links, free flow travel time of the links, distance of links, OD estimation, decision probability matrices, and the matrix of location of drivers.

The output is the optimized objective value of model (3) and total travel time and Carbon emission. This code should be run Python 3.

8. OptModel_linear2.py: The inputs are a YAML configuration file, graph of the network, free flow speed of links, capacity of links, free flow travel time of the links, distance of links, OD estimation, decision probability matrices, and the matrix of location of drivers. The output is the optimized objective value of model (4) and total travel time and Carbon emission. This code should be run Python 3.
9. run.py: The inputs are a YAML configuration file, graph of the network, speed of links, and volume of the links. The outputs are OD estimation, a matrix of travel time of each link, decision probability matrices, and the matrix of location of drivers. This code should be run on Linux and Python 2.

Here, we have provided a description of our data sets and we can share a sample of our run upon a reasonable request.

- YAML files are configuration files for each setting of optimization and OD estimation.
- congestion_inventory(original).csv: the information of sensors
- Mar2May_2018_new_5-22_link_capacity_region_x4_modified.csv: capacity of links in CSV format
- Mar2May_2018_new_5-22_link_capacity_region_x4_modified.pickle: capacity of links in pickle format
- Mar2May_2018_new_5-22_link_s_0_region_x4_modified.csv: free flow speed of links in mile per hour in CSV format
- Mar2May_2018_new_5-22_link_s_0_region_x4_modified.pickle: free flow speed of links mile per hour in pickle format
- Mar2May_2018_new_5-22_link_tt_0_hours_region_x4_modified.csv: free flow travel time of links in hour in CSV format
- Mar2May_2018_new_5-22_link_tt_0_hours_region_x4_modified.pickle: free flow travel time of links in hour in pickle format
- Mar2May_2018_new_5-22_link_tt_0_minutes_region_x4_modified.csv: free flow travel time of links in minutes in CSV format
- Mar2May_2018_new_5-22_link_tt_0_minutes_region_x4_modified. pickle: free flow travel time of links in minutes in pickle format
- Mar2May_2018_new_5-22_path_tt_minutes_region_x4_modified.pickle: free flow travel time of paths in minutes in pickle format
- Mar2May_2018_new_5-22_sensor_capacity_region_x4_modified.csv: capacity of sensors in CSV format
- Mar2May_2018_new_5-22_sensor_capacity_region_x4_modified.pickle: capacity of sensors in pickle format
- Mar2May_2018_new_5-22_sensor_s_0_region_x4_modified.csv: free flow speed of links in mile per hour in CSV format

- Mar2May_2018_new_5-22_sensor_s_0_region_x4_modified.pickle: free flow speed of links in mile per hour in pickle format
- AdjMatrix_region_x4_modified_original.csv: adjacency matrix of the network in CSV format
- link_length_meter_region_x4_modified_original.csv: length of the links in meter in CSV format
- link_length_meter_region_x4_modified_original.pickle: length of the links in meter in pickle format
- link_length_mile_region_x4_modified_original.csv: length of the links in mile in CSV format
- link_length_mile_region_x4_modified_original.pickle: length of the links in mile in pickle format
- my_graph_region_x4_modified_original.gpickle: graph of the network in pickle format
- my_ID_region_x4_modified_original.csv: ID of links in CSV format
- my_ID_region_x4_modified_original.pickle: ID of links in pickle format
- my_od_list_region_x4_modified_original.pickle: list of OD points of Experiment I in pickle format
- my_od_list_region_x4_modified_original_sub1.pickle: list of OD points of Experiment I in pickle format
- unique_sensors_region_x4_modified_original.pickle: list of sensors in pickle format
- AdjMatrix_region_x4_modified_original_Distance.csv: distance of links in miles in CSV format
- AdjMatrix_region_x4_modified_original_Distance. pickle: distance of links in miles in pickle format
- my_od_list_region_x4_modified_original_sub1.pickle: OD pairs of Experiment II in pickle format
- OD_list_region_x4_original_sub1.csv: list of OD points of Experiment II in CSV format
- 2018_Feb2Nov_location_table.csv: location of sensors in CSV format
- my_link_avg_count_data_AVG15min_5-10_region_x4_modified_pad.pickle: volume of links for 15 minutes intervals from 5 AM to 10 PM of March, April, May of 2018 in pickle format
- my_link_avg_spd_data_AVG15min_5-10_region_x4_modified_pad.pickle: speed of links for 15 minutes intervals from 5 AM to 10 PM of March, April, May of 2018 in pickle format
- sorted_IDs_Mar2May_2018_new_5-10_region_x4_modified_pad.csv: list of ID of sensors in CSV format
- speed_Mar2May_2018_new_5-10_region_x4_modified_pad.CSV: speed of sensors for 5 minutes intervals from 5 AM to 10 PM of March, April, May of 2018 in CSV format

- volume_Mar2May_2018_new_5-10_region_x4_modified_pad.csv: volume of sensors for 5 minutes intervals from 5 AM to 10 PM of March, April, May of 2018 in CSV format
- Outputs of OD estimation are saved in P_matrix_opt, Q_vector, R_matrix, tt, X_vector, and observe_index_N files. P_matrix_opt includes the decision probability matrices. Q_vector contains OD estimations. R_matrix includes the matrices of probability of location of drivers. X_vector includes lists of observed links from the network. Observe_index_N has index files of each link for running OD estimation.

Data Access and Sharing

The codes are free to share and open to the public. In particular, we have uploaded the codes on DRYAD platform (DOI https://doi.org/10.5061/dryad.ncjsxkst8). Moreover, we will share the code on the GitHub repository of the PI (https://github.com/optimization-for-data-driven-science).

As input to our codes, we used Archived Data Management System (ADMS) that collects, archives, and integrates a variety of transportation datasets from Los Angeles, Orange, San Bernardino, Riverside, and Ventura Counties. ADMS includes access to real-time traffic datasets from i) 9500 highway and arterial loop detectors providing data approximately every 1 minute, and ii) 2500 bus and train GPS location (AVL) data operating throughout Los Angeles County. We can share a sample of our run upon a reasonable request.

Results of this work will be published in peer- reviewed scientific journals, books published in English, conference proceedings, or as peer-reviewed data reports.

Reuse and Redistribution

USC's policy is to encourage, wherever appropriate, research data to be shared with the general public through internet access. This public access will be regulated by the university in order to protect privacy and confidentiality concerns, as well to respect any proprietary or intellectual property rights. Administrators will consult with the university's legal office to address any concerns on a case-by case basis, if necessary. Terms of use will include requirements of attribution along with disclaimers of liability in connection with any use or distribution of the research data, which may be conditioned under some circumstances.

Appendix

List of Notations

The following symbols are used in this report.

- G: Directed graph of traffic network
- V: Set of nodes of graph G which correspond to major intersections and ramps
- E: Set of edges of graph G which correspond the set of road segments
- e: An edge of graph G which corresponds to a road segments in the traffic network
- $|\mathrm{E}|$: Total number of road segments/edges in the network G (i.e. the cardinality of the set E)
- $\boldsymbol{r}$: Route vector
- $\boldsymbol{T}$: Time horizon
- $|\boldsymbol{T}|$:Number of time units (i.e. the cardinality of $\boldsymbol{T}$)
- t: One unit of time
- v_0: Capacity vector of road segments
- v_t: Volume vector of road segments at time t
- N: Set of drivers
- $|N|$: Number of drivers (i.e. the cardinality of the set N)
- R_n: Set of possible route options for driver n
- I_n: Set of possible incentives to offer to driver n
- $\mathrm{s_i^{r,n}}$: Decision parameter indicates whether incentive i is offered to driver n for route $\mathbf{r}$
- $\mathrm{p_i^{r,n}}$: The probability of acceptance of route $\mathbf{r}$ by driver n given incentive i
- $\hat{T}_r$: The estimate of the travel time for route $\mathbf{r}$ provided by the incentive offering platform
- T_r: Travel time for route $\mathbf{r}$
- $\beta_{r,t}$: The vector of location of driver that is driving in route $\mathbf{r}$ at time t

- q_i: The cost of incentive i
- $f_{CE}(.)$: Carbon emission function
- L: Length of the link
- $\mathbf{S}$: Decision matrix
- $\mathbf{R}$: The matrix of location of a driver
- $\mathbf{P}$: Route choice probability matrix
- $\mathbf{D}$: The matrix of incentive assignment to OD pairs
- $\mathbf{q}$: The vector of number of drivers for each OD pair
- $\mathbf{c}$: The vector of cost of incentives assigned to each route
- Ω: Budget

Robust Traffic Flow Prediction

In this section, we present the details of our speed prediction algorithm used as the input data in our optimization model. The prediction algorithm is based on a fully connected Neural Network with historical and real-time traffic data as input and the speed of next $|T|$ times ahead as output. The standard approach have been minimizing a loss function $\mathrm{l}(.)$ to learn a set of parameters w based on the observed data $(x_i, y_i), i = 1,2, \dots n$:

$$\min_{w} \sum_{i=1}^{n} \mathrm{l}\big((\boldsymbol{x_i}, \boldsymbol{y_i}), \boldsymbol{w}\big).$$

For simplicity, we define $f_i(w) := \mathrm{l}\big((x_i, y_i), w\big)$ and re-write the above training procedure as

$$\min_{w} \sum_{i=1}^{n} f_i(\boldsymbol{w}).$$

Previous studies such as [57] predict the traffic flow/speed based on the standard approach. Although the average error in the previous studies is small, there is no guarantee to have a small error for different road segments in the network. In fact, we observe that for some particular road segments the predictions are far from the actual values. This could significantly affect our next modeling steps by moving away or bringing a lot of drivers to those road segments. To make the error in our predictions more reliable, we suggest the following modification. Motivated by the concept of conditional-value-at-risk, we propose to minimize the average of the k worst prediction errors in the set of predictions. In particular, we formulate the problem as a min-max problem

$$\begin{aligned} \min_{\mathbf{w}} \max_{\mathbf{t}} \quad & \sum_{i=1}^{n} t_i f_i(\mathbf{w}) \\ \text{s.t.} \quad & \sum_{i=1}^{n} t_i = k, \\ & t_i \leq 1, \forall i = 1, 2, \ldots, n, \\ & t_i \geq 0, \forall i = 1, 2, \ldots, n. \end{aligned} \tag{11}$$

where w is the vector of weights of Neural Network and we want to minimize the loss function by learning them and $t \in [0,1]^k$ chooses the worst k predictions so we maximize the objective function w.r.t. t. The constraint $\sum_{i=1}^{n} t_i = k$ imposes the number of worst predictions.

Details of Alternating Direction Method of Multipliers (ADMM)

Before explaining the steps of our proposed algorithm, let us first explain Alternating Direction Method of Multipliers (ADMM), which is a main building block of our framework.

Review of ADMM

$$\min_{w,z} \quad h(w) + g(z) \qquad \text{s.t.} \quad Aw + Bz = c,$$

where $w \in R^{d_1}, z \in R^{d_2}$, $c \in R^k$, $A \in R^{k \times d_1}$, and $B \in R^{k \times d_2}$. By forming the augmented Lagrangian function

$$\mathcal{L}(w, z, \lambda) \triangleq h(w) + g(z) + \langle \lambda, Aw + Bz - c \rangle + \frac{\rho}{2} \|Aw + Bz - c\|_2^2,$$

each iteration of ADMM applies alternating minimization to the primal variables and gradient ascent to the dual variables. More precisely, at iteration r, ADMM uses the update rules:

$$\begin{aligned} \text{Primal Update:} \quad & w^{r+1} = \arg\min_{w} \mathcal{L}(w, z^r, \lambda^r), \\ & z^{r+1} = \arg\min_{z} \mathcal{L}(w^{r+1}, z, \lambda^r) \\ \text{Dual Update:} \quad & \lambda^{r+1} = \lambda^r + \rho \left(Aw^{r+1} + Bz^{r+1} - c \right) \end{aligned} \tag{16}$$

This algorithm is well studied in the optimization literature (see [71] for a monograph on the us of this algorithm in convex distributed optimization, [74] for its use in non-convex continuous optimization, and [85] for its application in discrete optimization).

ADMM for Solving (9)

Let

$$\begin{aligned}\mathcal{L}(\boldsymbol{\gamma},\mathbf{S},\mathbf{H},\mathbf{W},\mathbf{u},\beta) \triangleq & \sum_{\gamma_{\ell,t}} f_{CE}(\gamma_{\ell,t}) + \mathbb{I}_{[0,1]^{(|\mathcal{R}|\cdot|\mathcal{I}|)\times|\mathcal{N}|}}(\mathbf{H}) + \mathbb{I}_{\mathbb{R}^+}(\beta) + <\boldsymbol{\lambda}_1, \mathbf{S}\mathbf{1}-\mathbf{u}> + \\ & <\boldsymbol{\lambda}_2, \mathbf{W}^\intercal\mathbf{1}> + <\boldsymbol{\lambda}_3, \mathbf{D}\mathbf{u}-\mathbf{q}> + <\boldsymbol{\lambda}_4, \mathbf{A}\mathbf{u}-\boldsymbol{\gamma}> + \\ & <\boldsymbol{\lambda}_5, \mathbf{H}-\mathbf{S}> + \lambda_6(\mathbf{c}^\intercal\mathbf{u}+\beta-\Omega) + <\boldsymbol{\lambda}_7, \mathbf{W}-\mathbf{S}> + \\ & \frac{\rho}{2}||\mathbf{S}\mathbf{1}-\mathbf{u}||^2 + \frac{\rho}{2}||\mathbf{H}-\mathbf{S}||^2 + \frac{\rho}{2}||\mathbf{W}^\intercal\mathbf{1}-\mathbf{1}||^2 + \\ & \frac{\rho}{2}||\mathbf{D}\mathbf{u}-\mathbf{q}||^2 + \frac{\rho}{2}||\mathbf{A}\mathbf{u}-\boldsymbol{\gamma}||^2 + \frac{\rho}{2}(\mathbf{c}^\intercal\mathbf{u}+\beta-\omega)^2 + \\ & \frac{\rho}{2}||\mathbf{W}-\mathbf{S}||^2\end{aligned}$$

be the augmented Lagrangian function of model (10) with the set of Lagrange multipliers $\{\lambda_1, \lambda_2, \ldots, \Lambda_7\}$ and $\rho > 0$ be the primal penalty parameter. Then, ADMM solves model (10) by the following iterative scheme

$$\text{(ADMM)} \begin{cases} \mathbf{u}^{t+1} = & \underset{\mathbf{u}}{\operatorname{argmin}} \quad <\boldsymbol{\lambda}_1^t, \mathbf{S}^{t+1}\mathbf{1}-\mathbf{u}> + <\boldsymbol{\lambda}_3^t, \mathbf{D}\mathbf{u}-\mathbf{q}> + <\boldsymbol{\lambda}_4^t, \mathbf{A}\mathbf{u}-\boldsymbol{\gamma}> + \\ & \frac{\rho}{2}||\mathbf{S}^{t+1}\mathbf{1}-\mathbf{u}||^2 + \frac{\rho}{2}||\mathbf{D}\mathbf{u}-\mathbf{q}||^2 + \frac{\rho}{2}||\mathbf{A}\mathbf{u}-\boldsymbol{\gamma}||^2 \\ \mathbf{W}^{t+1} = & \underset{\mathbf{W}}{\operatorname{argmin}} \quad <\boldsymbol{\lambda}_2^t, \mathbf{W}^\intercal-\mathbf{1}> + <\boldsymbol{\Lambda}_7^t, \mathbf{W}-\mathbf{S}^{t+1}> + \frac{\rho}{2}||\mathbf{W}^\intercal\mathbf{1}-\mathbf{1}||^2 + \\ & \frac{\rho}{2}||\mathbf{W}-\mathbf{S}^{t+1}||^2 \\ \mathbf{H}^{t+1} = & \underset{\mathbf{H}}{\operatorname{argmin}} \quad \mathbb{I}_{[0,1]}(\mathbf{H}) + <\boldsymbol{\Lambda}_5^t, \mathbf{H}-\mathbf{S}^{t+1}> + \frac{\rho}{2}||\mathbf{H}-\mathbf{S}^{t+1}||^2 \\ \mathbf{S}^{t+1} = & \underset{\mathbf{S}}{\operatorname{argmin}} \quad <\boldsymbol{\lambda}_1^t, \mathbf{S}\mathbf{1}-\mathbf{u}^t> + <\boldsymbol{\lambda}_5^t, \mathbf{H}^t-\mathbf{S}> + <\boldsymbol{\lambda}_7^t, \mathbf{W}^t-\mathbf{S}> + \\ & \frac{\rho}{2}||\mathbf{S}\mathbf{1}-\mathbf{u}^t||^2 + \frac{\rho}{2}||\mathbf{H}^t-\mathbf{S}||^2 + \frac{\rho}{2}||\mathbf{W}^t-\mathbf{S}||^2 \\ \beta^{t+1} = & \underset{\beta}{\operatorname{argmin}} \quad \mathbb{I}_+(\beta) + \lambda_6^t(\mathbf{c}^\intercal\mathbf{u}^{t+1}+\beta-\Omega) + \frac{\rho}{2}(\mathbf{c}^\intercal\mathbf{u}^{t+1}+\beta-\Omega)^2 \\ \boldsymbol{\lambda}_1^{t+1} = & \boldsymbol{\lambda}_1^t + \rho(\mathbf{S}^{t+1}\mathbf{1}-\mathbf{u}^{t+1}) \\ \boldsymbol{\lambda}_2^{t+1} = & \boldsymbol{\lambda}_2^t + \rho(\mathbf{W}^{t+1\intercal}\mathbf{1}-\mathbf{1}) \\ \boldsymbol{\lambda}_3^{t+1} = & \boldsymbol{\lambda}_3^t + \rho(\mathbf{D}\mathbf{u}^{t+1}-\mathbf{q}) \\ \boldsymbol{\lambda}_4^{t+1} = & \boldsymbol{\lambda}_4^t + \rho(\mathbf{A}\mathbf{u}^{t+1}-\boldsymbol{\gamma}^{t+1}) \\ \boldsymbol{\Lambda}_5^{t+1} = & \boldsymbol{\Lambda}_5^t + \rho(\mathbf{H}^{t+1}-\mathbf{S}^{t+1}) \\ \lambda_6^{t+1} = & \lambda_6^t + \rho(\mathbf{c}^\intercal\mathbf{u}^{t+1}+\beta^{t+1}-\Omega) \\ \boldsymbol{\Lambda}_7^{t+1} = & \boldsymbol{\Lambda}_7^t + \rho(\mathbf{W}^{t+1}-\mathbf{S}^{t+1}) \end{cases} \tag{17}$$

The gradient of the differentiable part of Lagrangian function w.r.t. variables S, H, W, u, and β can be computed as:

$$
\begin{cases}
\frac{\partial \mathcal{L}}{\partial \mathbf{u}} = & -\boldsymbol{\lambda}_1 + \mathbf{D}^\intercal \boldsymbol{\lambda}_3 + \mathbf{A}^\intercal \boldsymbol{\lambda}_4 + \mathbf{c}\boldsymbol{\Lambda}_6 \rho\left(\mathbf{u} - \mathbf{S}\mathbf{1}\right) + \rho \mathbf{D}^\intercal\left(\mathbf{D}\mathbf{u} - \mathbf{q}\right) + \rho \mathbf{A}^\intercal\left(\mathbf{A}\mathbf{u} - \boldsymbol{\gamma}\right) + \\
& \rho \mathbf{c}(\mathbf{c}^\intercal \mathbf{u} + \beta - \Omega) \\
\frac{\partial \mathcal{L}}{\partial \mathbf{W}} = & \mathbf{1}\boldsymbol{\lambda}_2^\intercal + \boldsymbol{\Lambda}_9 + \rho \mathbf{1}\left(\mathbf{W}^\intercal \mathbf{1} - \mathbf{1}\right)^\intercal + \rho\left(\mathbf{W} - \mathbf{S}\right) \\
\frac{\partial \mathcal{L}}{\partial \mathbf{H}} = & \boldsymbol{\Lambda}_5 + \rho\left(\mathbf{H} - \mathbf{S}\right) \\
\frac{\partial \mathcal{L}}{\partial \mathbf{S}} = & \boldsymbol{\lambda}_1 \mathbf{1}^\intercal - \boldsymbol{\lambda}_5 - \boldsymbol{\lambda}_7 + \rho(\mathbf{S}\mathbf{1} - \mathbf{u})\mathbf{1}^\intercal + \rho\left(\mathbf{S} - \mathbf{H}\right) + \rho\left(\mathbf{S} - \mathbf{W}\right) \\
\frac{\partial \mathcal{L}}{\partial \beta} = & \lambda_7 + \rho\left(\mathbf{c}^\intercal \mathbf{u} + \beta - \Omega\right)
\end{cases} \tag{18}
$$

Then the updates for primal variables are described as follows:

$$
\begin{cases}
\gamma_{\ell,\hat{t}}^{t+1} = & \underset{\gamma_{\ell,\hat{t}}}{\operatorname{argmin}}\, \gamma_{\ell,\hat{t}} f_{CE}\left(\delta(\gamma_{\ell,\hat{t}})\right) L_\ell + \boldsymbol{\lambda}_{4,(\ell,\hat{t})}^t(\mathbf{a}_{\ell,\hat{t}}\mathbf{u}^t - \gamma_{\ell,\hat{t}}) + \frac{\rho}{2}(\mathbf{a}_{\ell,\hat{t}}\mathbf{u}^t - \gamma_{\ell,\hat{t}})^2, \quad \forall \ell, \forall \hat{t} \\
\mathbf{S}^{t+1} = & \frac{1}{\rho}(-\boldsymbol{\lambda}_1^t \mathbf{1}^\intercal + \boldsymbol{\Lambda}_5^t + \boldsymbol{\Lambda}_9^t + \rho \mathbf{u}^t \mathbf{1}^\intercal + \rho \mathbf{H}^t + \rho \mathbf{W}^t)(\mathbf{1}\mathbf{1}^\intercal + 2\mathbf{I})^{-1} \\
\boldsymbol{\theta}^{t+1} = & \frac{1}{\rho}(\mathbf{I} + \mathbf{c}^t \mathbf{c}^{t\intercal})^{-1}(-\boldsymbol{\lambda}_6^t - \lambda_7^t \mathbf{c}^t + \rho \mathbf{u}^t - \rho \beta^t \mathbf{c}^t + \rho \Omega \mathbf{c}^t) \\
\mathbf{z}^{t+1} = & \frac{1}{\rho}(\boldsymbol{\lambda}_8^t + \rho \mathbf{u}^t) \\
\mathbf{H}^{t+1} = & \Pi\Big(\frac{1}{\rho}(-\boldsymbol{\Lambda}_5^t + \rho \mathbf{S}^{t+1})\Big)_{[0,1]} \\
\mathbf{W}^{t+1} = & \frac{1}{\rho}(\mathbf{I} + \mathbf{1}\mathbf{1}^\intercal)^{-1}(-\mathbf{1}\boldsymbol{\lambda}_2^{t\intercal} - \boldsymbol{\Lambda}_9^t + \rho \mathbf{1}\mathbf{1}^\intercal + \rho \mathbf{S}^{t+1}) \\
\mathbf{u}^{t+1} = & \frac{1}{\rho}(3\mathbf{I} + \mathbf{D}^\intercal \mathbf{D} + \mathbf{A}^\intercal \mathbf{A})^{-1}(\boldsymbol{\lambda}_1^t - \mathbf{D}^\intercal \boldsymbol{\lambda}_3^t - \mathbf{A}^\intercal \boldsymbol{\lambda}_4^t + \boldsymbol{\lambda}_6^t - \boldsymbol{\lambda}_8^t + \rho \mathbf{S}^{t+1}\mathbf{1} + \rho \mathbf{D}^\intercal \mathbf{q} + \\
& \rho \mathbf{A}^\intercal \boldsymbol{\gamma}^{t+1} + \rho \mathbf{u}^{t+1} + \rho \mathbf{z}^{t+1}) \\
\beta^{t+1} = & \Pi\left(\frac{1}{\rho}(-\lambda_7^t - \rho \mathbf{c}^{t\intercal}\mathbf{u}^t + \rho \Omega)\right)_{\mathbb{R}_+}
\end{cases} \tag{19}
$$

Q-ADMM for Rounding the Solution of (9)

The formulation of our ADMM-Q method can simply be derived from the formulation of model (9) by adding two constraints for **Q**:

$$
\begin{aligned}
\min_{\boldsymbol{\gamma},\mathbf{u},\mathbf{S},\mathbf{W},\mathbf{H},\mathbf{z},\beta} \quad & \sum_{\ell=1}^{|\mathcal{E}|}\sum_{t=1}^{|\mathbf{T}|} \gamma_{\ell,t} f_{CE}\left(\delta(\gamma_{\ell,t})\right) L_\ell \\
\text{s.t.} \quad & \mathbf{S}\mathbf{1} = \mathbf{u}, \quad \mathbf{W}^\intercal \mathbf{1} = \mathbf{1} \\
& \mathbf{D}\mathbf{u} = \mathbf{q}, \quad \mathbf{A}\mathbf{u} = \boldsymbol{\gamma} \\
& \mathbf{H} = \mathbf{S}, \quad \mathbf{W} = \mathbf{S} \\
& \mathbf{c}^\intercal \mathbf{u} + \beta = \Omega, \quad \beta \geq 0 \\
& \mathbf{H} \in [0,1]^{(|\mathcal{R}|\cdot|\mathcal{I}|)\times|\mathcal{N}|} \\
& \mathbf{Q} = \mathbf{S}, \mathbf{Q} \in \{0,1\}^{(|\mathcal{R}|\cdot|\mathcal{I}|)\times|\mathcal{N}|}
\end{aligned} \tag{20}
$$

Let

$$\mathcal{L}(\gamma, \mathbf{S}, \mathbf{H}, \mathbf{W}, \mathbf{u}, \beta, \mathbf{Q}) \triangleq \sum_{\gamma_{\ell,t}} f_{CE}(\gamma_{\ell,t}) + \mathbb{I}_{[0,1]^{(|\mathcal{R}|\cdot|\mathcal{I}|)\times|\mathcal{N}|}}(\mathbf{H}) + \mathbb{I}_{\mathbb{R}^+}(\beta) + \mathbb{I}_{\{0,1\}^{(|\mathcal{R}|\cdot|\mathcal{I}|)\times|\mathcal{N}|}}(\mathbf{Q}) +$$
$$< \boldsymbol{\lambda}_1, \mathbf{S1} - \mathbf{u} > + < \boldsymbol{\lambda}_2, \mathbf{W}^\intercal \mathbf{1} > + < \boldsymbol{\lambda}_3, \mathbf{Du} - \mathbf{q} > + < \boldsymbol{\lambda}_4, \mathbf{Au} - \boldsymbol{\gamma} > +$$
$$< \boldsymbol{\lambda}_5, \mathbf{H} - \mathbf{S} > + \lambda_6(\mathbf{c}^\intercal \mathbf{u} + \beta - \Omega) + < \boldsymbol{\lambda}_7, \mathbf{W} - \mathbf{S} > + < \boldsymbol{\lambda}_8, \mathbf{Q} - \mathbf{S} > +$$
$$\frac{\rho}{2}||\mathbf{S1} - \mathbf{u}||^2 + \frac{\rho}{2}||\mathbf{H} - \mathbf{S}||^2 + \frac{\rho}{2}||\mathbf{W}^\intercal \mathbf{1} - \mathbf{1}||^2 +$$
$$\frac{\rho}{2}||\mathbf{Du} - \mathbf{q}||^2 + \frac{\rho}{2}||\mathbf{Au} - \boldsymbol{\gamma}||^2 + \frac{\rho}{2}(\mathbf{c}^\intercal \mathbf{u} + \beta - \omega)^2 +$$
$$\frac{\rho}{2}||\mathbf{W} - \mathbf{S}||^2 + \frac{\rho}{2}||\mathbf{Q} - \mathbf{S}||^2$$

be the augmented Lagrangian function of model (20) with the set of Lagrange multipliers $\{\lambda_1, \lambda_2, \ldots, \Lambda_8\}$ and $\rho > 0$ be the primal penalty parameter. Then, ADMM-Q solves model (20) by an iterative scheme similar to (17) in which only update rule of S is different:

$$\mathbf{S}^{t+1} = \underset{\mathbf{S}}{\operatorname{argmin}} \quad < \boldsymbol{\lambda}_1^t, \mathbf{S1} - \mathbf{u}^t > + < \boldsymbol{\lambda}_5^t, \mathbf{H}^t - \mathbf{S} > + < \boldsymbol{\lambda}_7^t, \mathbf{W}^t - \mathbf{S} > +$$
$$\frac{\rho}{2}||\mathbf{S1} - \mathbf{u}^t||^2 + \frac{\rho}{2}||\mathbf{H}^t - \mathbf{S}||^2 + \frac{\rho}{2}||\mathbf{W}^t - \mathbf{S}||^2 + < \boldsymbol{\Lambda}_8, \mathbf{Q}^t - \mathbf{S} > + \frac{\rho}{2}||\mathbf{Q}^t - \mathbf{S}||^2$$

and we have an update rule for the new variable Q:

$$\mathbf{Q}^{t+1} = \underset{\mathbf{Q}}{\operatorname{argmin}} \quad < \boldsymbol{\Lambda}_8, \mathbf{Q} - \mathbf{S} > + \frac{\rho}{2}||\mathbf{Q} - \mathbf{S}||^2 + \mathbb{I}_{\{0,1\}^{(|\mathcal{R}|\cdot|\mathcal{I}|)\times|\mathcal{N}|}}(\mathbf{Q})$$

The gradient of the differentiable part of Lagrangian function w.r.t. variables H, W, u, and β are similar to and the gradient w.r.t. S and Q can be computed as:

$$\begin{cases} \frac{\partial \mathcal{L}}{\partial \mathbf{S}} = & \boldsymbol{\lambda}_1 \mathbf{1}^\intercal - \boldsymbol{\lambda}_5 - \boldsymbol{\lambda}_7 + \rho(\mathbf{S1} - \mathbf{u})\mathbf{1}^\intercal + \rho\,(\mathbf{S} - \mathbf{H}) + \rho\,(\mathbf{S} - \mathbf{W}) - \boldsymbol{\Lambda}_8 + \rho(\mathbf{S} - \mathbf{Q}) \\ \frac{\partial \mathcal{L}}{\partial \mathbf{Q}} = & \boldsymbol{\Lambda}_8 + \rho(\mathbf{Q} - \mathbf{S}) \end{cases}$$

Then the updates for primal variables u, z, H, W, u, and β are similar to (19) and the updates of S and Q are described as follows:

$$\begin{cases} \mathbf{S}^{t+1} = & \frac{1}{\rho}(-\boldsymbol{\lambda}_1^t \mathbf{1}^\intercal + \boldsymbol{\Lambda}_5^t + \boldsymbol{\Lambda}_7^t + \rho \mathbf{u}^t \mathbf{1}^\intercal + \rho \mathbf{H}^t + \rho \mathbf{W}^t + \boldsymbol{\Lambda}_8^t + \rho \mathbf{Q})(\mathbf{1}\mathbf{1}^\intercal + 3\mathbf{I})^{-1} \\ \mathbf{Q}^{t+1} = & \Pi\left(\mathbf{S}^{t+1} - \frac{1}{\rho}\boldsymbol{\Lambda}_8^t\right)_{\{0,1\}^{(|\mathcal{R}|\cdot|\mathcal{I}|)\times|\mathcal{N}|}} \end{cases}$$

The steps of ADMM-Q algorithm are summarized in Algorithm 2.

Algorithm 2 ADMM-Q

Input: Initial values: $\boldsymbol{\gamma}^0$, $\mathbf{S}^0$, $\mathbf{H}^0$, $\mathbf{W}^0$, $\mathbf{u}^0$, β^0, $\boldsymbol{\lambda}_1^0 \in \mathbb{R}^{|\mathcal{R}|\cdot|\mathcal{I}|\times 1}$, $\boldsymbol{\lambda}_2^0 \in \mathbb{R}^{|\mathcal{N}|\times 1}$, $\boldsymbol{\lambda}_3^0 \in \mathbb{R}^{K\times 1}$, $\boldsymbol{\lambda}_4^0 \in \mathbb{R}^{|\mathcal{E}|\cdot\mathbf{T}\times 1}$, $\boldsymbol{\Lambda}_5^0 \in \mathbb{R}^{|\mathcal{R}|\cdot|\mathcal{I}|\times|\mathcal{N}|}$, $\lambda_6^0 \in \mathbb{R}$, $\boldsymbol{\Lambda}_7^0 \in \mathbb{R}^{|\mathcal{R}|\cdot|\mathcal{I}|\times|\mathcal{N}|}$, $\boldsymbol{\Lambda}_8^0 \in \mathbb{R}^{|\mathcal{R}|\cdot|\mathcal{I}|\times|\mathcal{N}|}$, Dual update step: ρ, Number of iterations: T.

for $t = 0, 1, \ldots, T$ **do**

$\mathbf{u}^{t+1} = (\rho\mathbf{I} + \rho\mathbf{D}^\intercal\mathbf{D} + \rho\mathbf{A}^\intercal\mathbf{A} + \rho\mathbf{c}\mathbf{c}^\intercal)^{-1}(\boldsymbol{\lambda}_1^t + \rho\mathbf{S}^t\mathbf{1} - \mathbf{D}^\intercal\boldsymbol{\lambda}_3^t + \rho\mathbf{D}^\intercal\mathbf{q} - \mathbf{A}^\intercal\boldsymbol{\lambda}_4^t + \rho\mathbf{A}^\intercal\boldsymbol{\gamma}^t - \mathbf{c}(\lambda_6^t + \beta^t - \Omega))$

$\mathbf{W}^{t+1} = (\rho\mathbf{1}\mathbf{1}^\intercal + \rho\mathbf{I})^{-1}(\rho\mathbf{1}\mathbf{1}^\intercal + \rho\mathbf{S}^t - \boldsymbol{\Lambda}_7^t - \mathbf{1}\boldsymbol{\lambda}_2^{t\intercal})$

$\mathbf{H}^{t+1} = \Pi\left(\mathbf{S}^t - \frac{1}{\rho}\boldsymbol{\Lambda}_5^t\right)_{[0,1]}$

$\mathbf{Q}^{t+1} = \Pi\left(\mathbf{S}^{t+1} - \frac{1}{\rho}\boldsymbol{\Lambda}_8^t\right)_{\{0,1\}^{(|\mathcal{R}|\cdot|\mathcal{I}|)\times|\mathcal{N}|}}$

$\mathbf{S}^{t+1} = (\rho\mathbf{u}^{t+1}\mathbf{1}^\intercal + \boldsymbol{\Lambda}_5^t + \rho\mathbf{H}^{t+1} + \boldsymbol{\Lambda}_7^t + \rho\mathbf{W}^{t+1} - \boldsymbol{\lambda}_1^t\mathbf{1}^\intercal)(\rho\mathbf{1}\mathbf{1}^\intercal + 3\rho\mathbf{I})^{-1}$

for $\ell = 0, 1, \ldots, |\mathcal{E}|$ **do**

for $\hat{t} = 1, \ldots, |\mathbf{T}|$ **do**

$\boldsymbol{\gamma}_{\ell,\hat{t}}^{t+1} = \underset{\boldsymbol{\gamma}_{\ell,\hat{t}}}{\operatorname{argmin}}\, \boldsymbol{\gamma}_{\ell,\hat{t}} f_{CE}\left(\delta(\boldsymbol{\gamma}_{\ell,\hat{t}})\right) L_\ell + \boldsymbol{\lambda}_{4,(\ell,\hat{t})}^t(\mathbf{a}_{\ell,\hat{t}}\mathbf{u}^t - \boldsymbol{\gamma}_{\ell,\hat{t}}) + \frac{\rho}{2}(\mathbf{a}_{\ell,\hat{t}}\mathbf{u}^t - \boldsymbol{\gamma}_{\ell,\hat{t}})^2$

end for

end for

$\beta^{t+1} = \Pi\left(\Omega - \mathbf{c}^\intercal\mathbf{u}^{t+1} - \frac{1}{\rho}\lambda_6^t\right)_{\mathbb{R}_+}$

$\boldsymbol{\lambda}_1^{t+1} = \boldsymbol{\lambda}_1^t + \rho(\mathbf{S}^{t+1}\mathbf{1} - \mathbf{u}^{t+1})$

$\boldsymbol{\lambda}_2^{t+1} = \boldsymbol{\lambda}_2^t + \rho(\mathbf{W}^{t+1\intercal}\mathbf{1} - \mathbf{1})$

$\boldsymbol{\lambda}_3^{t+1} = \boldsymbol{\lambda}_3^t + \rho(\mathbf{D}\mathbf{u}^{t+1} - \mathbf{q})$

$\boldsymbol{\lambda}_4^{t+1} = \boldsymbol{\lambda}_4^t + \rho(\mathbf{A}\mathbf{u}^{t+1} - \boldsymbol{\gamma}^{t+1})$

$\boldsymbol{\Lambda}_5^{t+1} = \boldsymbol{\Lambda}_5^t + \rho(\mathbf{H}^{t+1} - \mathbf{S}^{t+1})$

$\lambda_6^{t+1} = \lambda_6^t + \rho(\mathbf{c}^\intercal\mathbf{u}^{t+1} + \beta^{t+1} - \Omega)$

$\boldsymbol{\Lambda}_7^{t+1} = \boldsymbol{\Lambda}_7^t + \rho(\mathbf{W}^{t+1} - \mathbf{S}^{t+1})$

$\boldsymbol{\Lambda}_8^{t+1} = \boldsymbol{\Lambda}_8^t + \rho(\mathbf{Q}^{t+1} - \mathbf{S}^{t+1})$

end for

Return: $\mathbf{S}^T$

An Example of the Model and Notations

In this section, we provide a small example of a network to illustrate our model and notations. Consider the following network

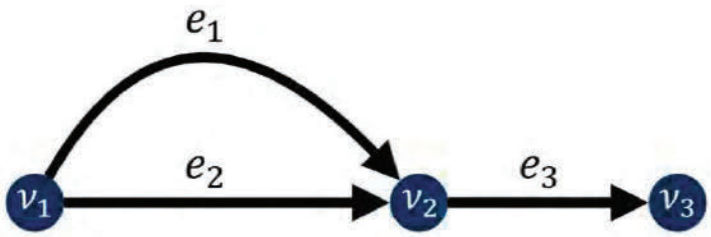

Figure 7. Network example G_1

where $\mathcal{V} = \{v_1, v_2, v_3\}$ is the set of nodes and $\mathcal{E} = \{e_1, e_2, e_3\}$ is the set edges (roads). Details of setting of links is represented Table 13. The (origin, destination) pair is (v_1, v_3). There are two routes going from origin to destination so $\mathcal{R} = \{r_1, r_2\}$. Each route is represented as $r = \{0,1\}^3$ where i^{th} element corresponds to e_i. Setting of routes is provided Table 14.

Table 27: Set of edges.

	Capacity	Length (Km)	Speed at free flow (Km/h)	Travel time at free flow (h)
e_1	1	10	50	0.2
e_2	1	5	50	0.1
e_3	2	5	50	0.1

Table 28: Set of routes.

	Links	r	Graph
Route 1	$e_2 \rightarrow e_3$	$r_1 = \begin{bmatrix} 0 \\ 1 \\ 1 \end{bmatrix}$	
Route 2	$e_1 \rightarrow e_3$	$r_1 = \begin{bmatrix} 1 \\ 0 \\ 1 \end{bmatrix}$	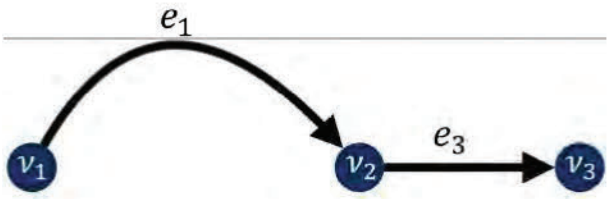

In this example, the time horizon set is $T = \{1,2,3\}$. The speed in all three times is equal to the speed at free flow of the links. To estimate the location of drivers at each time, we need matrix $R \in [0,1]^{9\times 6}$ as follows

$$\mathbf{R} = \begin{array}{c} \\ t_2=1,e_1 \\ t_2=1,e_2 \\ t_2=1,e_3 \\ t_2=2,e_1 \\ t_2=2,e_2 \\ t_2=2,e_3 \\ t_2=3,e_1 \\ t_2=3,e_2 \\ t_2=3,e_3 \end{array} \begin{array}{c} \begin{array}{cccccc} t_1=1,\mathbf{r}_1 & t_1=1,\mathbf{r}_2 & t_1=2,\mathbf{r}_1 & t_1=2,\mathbf{r}_2 & t_1=3,\mathbf{r}_1 & t_1=3,\mathbf{r}_2 \end{array} \\ \begin{pmatrix} 0 & 1 & 0 & 0 & 0 & 0 \\ 1 & 0 & 0 & 0 & 0 & 0 \\ 0 & 0 & 0 & 0 & 0 & 0 \\ 0 & 1 & 0 & 1 & 0 & 0 \\ 0 & 0 & 1 & 0 & 0 & 0 \\ 1 & 0 & 0 & 0 & 0 & 0 \\ 0 & 0 & 0 & 1 & 0 & 1 \\ 0 & 0 & 0 & 0 & 1 & 0 \\ 0 & 1 & 1 & 0 & 0 & 0 \end{pmatrix} \end{array}$$

where t_1 is the entrance time of the driver and t_2 is the driver's arrival time at the road. In model (3) and (4), the column vector $\beta_{r,t}$ corresponds to the columns of matrix R. For instance, the first column is $\beta_{r_1,t_1=1}$.

Assume there are two drivers in the system and $\mathcal{N} = \{d_1, d_2\}$. We want to offer rewards from the set $\mathcal{I} = \{0,$ to control the traffic. To estimate the probability of choosing routes given an offered incentive at a time, we use matrix $P \in [0,1]^{6\times 12}$ when incentive i is offered:

$$\mathbf{P}_{t_i} = \begin{array}{c} \\ t=1,\mathbf{r}_1 \\ t=1,\mathbf{r}_2 \\ t=2,\mathbf{r}_1 \\ t=2,\mathbf{r}_2 \\ t=3,\mathbf{r}_1 \\ t=3,\mathbf{r}_2 \end{array} \begin{array}{c} \begin{array}{cccc} \text{No incentive} & & \$5 \to \mathbf{r}_1 & \$5 \to \mathbf{r}_2 \end{array} \\ \begin{pmatrix} 0.63 & 0.63 & 0.98 & 0.05 \\ 0.37 & 0.37 & 0.2 & 0.95 \\ 0.63 & 0.63 & 0.98 & 0.05 \\ 0.37 & 0.37 & 0.2 & 0.95 \\ 0.63 & 0.63 & 0.98 & 0.05 \\ 0.37 & 0.37 & 0.2 & 0.95 \end{pmatrix} \end{array}, \quad \forall i \in \{1,2,3\}$$

$$\mathbf{P} = \begin{bmatrix} \mathbf{P}_{t_1} & \mathbf{P}_{t_2} & \mathbf{P}_{t_3} \end{bmatrix} \tag{21}$$

Probability matrices for all three times are equal because the speed is the same in all three times. We compute the probability of choosing route k given that $\$i'$ is offered for route j' by the driver as follows:

$$\mathbb{P}(\mathbf{r}=k, i=(\$i' \to \text{route } j')) = \frac{\exp\left(tt_k \times -0.086 + i' \times 0.7 \times \mathbb{I}_{k=j'}\right)}{\exp\left(tt_{j'} \times -0.086 + i' \times 0.7\right) + \sum_{j\neq j'} \exp\left(tt_j \times -0.086\right)} \tag{22}$$

where tt_j is the travel time of route j.

Notations in model (8):

$$\mathbf{D} = \begin{array}{c} \\ \text{OD } 1 \end{array} \begin{array}{c} \begin{array}{cccc} i=\$0,\mathbf{r}_1 & & i=\$0,\mathbf{r}_2 & i=\$5,\mathbf{r}_1 \end{array} \quad i=\$5,\mathbf{r}_2 \\ \begin{pmatrix} 1 & 1 & 1 & 1 \end{pmatrix} \end{array}$$

$$\mathbf{c} = \begin{matrix} \$0 \to \mathbf{r}_1 \\ \$0 \to \mathbf{r}_2 \\ \$5 \to \mathbf{r}_1 \\ \$5 \to \mathbf{r}_2 \end{matrix} \begin{pmatrix} 0 \\ 0 \\ 5 \\ 5 \end{pmatrix}$$

q vector is a scalar in this example and is equal to 2.

Convexity of the CO_2 Emission Function

The CO_2 emission function is:

$$f_{CO_2}(\delta) = a_0 - a_1 \cdot \delta + a_2 \cdot \delta^2 - a_3 \cdot \delta^3 + a_4 \cdot \delta^4$$

where the value of the coefficients are in the following table:

Table 29: Parameter values.

Parameter	a_0	a_1	a_2	a_3	a_4
Value	523.7	1654.4×10^{-2}	2635.4×10^{-4}	1771.5×10^{-6}	442.9×10^{-8}

In this project the input variable of the emission function is the output of the BPR function:

$$g(v) = \frac{L}{f_{BPR}(v)} = \frac{L}{t_0}\left(\beta_0 + \beta_1\left(\frac{v}{w}\right)^4\right)^{-1}$$

where w is the capacity of the link, t_0 is the free flow travel time of the link in hour, L is the length of the link in km, v is the volume of the link as input, $\beta_0 = 1$, and $\beta_1 = 0.15$. $\frac{L}{t_0}$ is the free flow speed of the link and we can rewrite the function as follows:

$$g(v) = c_0(\beta_0 + \beta_2 v^4)^{-1}$$

where c_0 is the free flow speed of the link and $\beta_2 = \frac{\beta_1}{w^4}$. The output of function $g(v)$ is the speed of the link. δ as input of CO_2 emission function is the output of the BPR function and we can rewrite the Emission function as:

$$f'_{CO_2}(v) = a_0 - a_1 \cdot g(v) + a_2 \cdot g(v)^2 - a_3 \cdot g(v)^3 + a_4 \cdot g(v)^4$$

To compute the second order derivative of $f_{CO_2}(v)$ we need the first order and second order derivative of $g(v)$:

$$g'(v) = \frac{-4c_0\beta_2 v^3}{(\beta_0 + \beta_2 v^4)^2}$$

$$g''(v) = \frac{4c_0\beta_2 v^2(5\beta_2 v^4 - 3\beta_0)}{(\beta_0 + \beta_2 v^4)^3}$$

Now, we can compute the first and second order derivatives of the function $f'_{CO_2}(v)$:

$$f'_{CO_2}(v) = a_0 + a_1 g(v) + a_1 v g'(v) + a_2 g^2(v) + 2a_2 v g(v) g'(v) + a_3 g^3(v) + 3a_3 v g^2(v) g'(v) + a_4 g(v)^4 + 4a_4 v g^3(v) g'(v)$$

$$f''_{CO_2}(v) = a_1 g''(v) + a_1 g'(v) + a_1 v g''(v) + 2a_2 g(v) g'(v) + 2a_2\big(v g'(v) + g(v)\big)(v) + 2a_2 v g(v) g''(v) + 3a_3 g(v)^2 g'(v) + 3a_3\big(g(v)^2 + 2v g(v) g'(v)\big) g'(v) + 3a_3 v g(v)^2 g''(v) + 4a_4 g^3(v) g'(v) + 4a_4\big(g^3(v) + 3v g^2(v) g'(v)\big) g'(v) + 4a_4 v g^3(v) g''(v)$$

To plot $f''_{CO_2}(v)$, we need two parameters: capacity of the link (w) and the free flow speed of the link (c_0). We consider the average of these two values from all the links so $w = 29$ and $c_0 = 46.27$ km/h. The second order derivative of the CO_2 emission function is depicted in Figure 6 based on the average of the capacity of the links and average of the free flow speed of the links so $w = 29$ and $c_0 = 46.27$ km/h. The plot shows the convexity of the function for $v \leq 64$ which is more than two times of the average of the capacities. Therefore, for $\alpha \leq 2.0$, on average we have convexity for the defined CO_2 emission function.

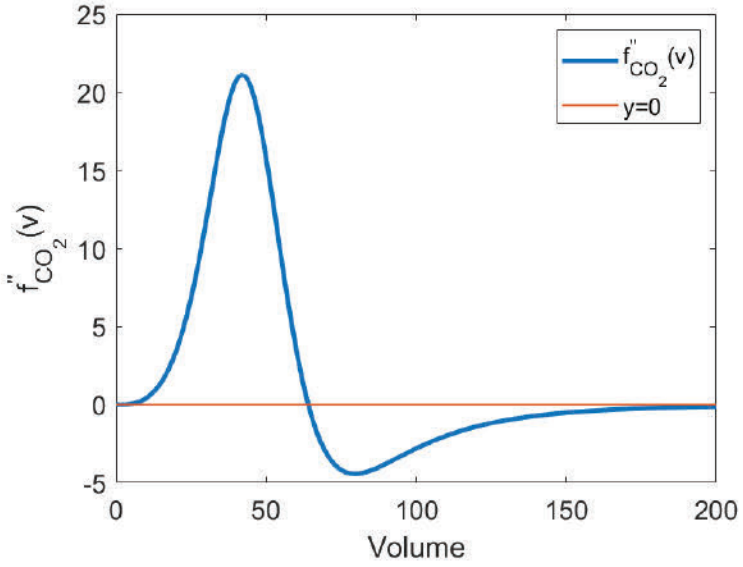

Figure 8. Second order derivative of CO_2 emission function

Details of the Numerical Results

Table 30: Distribution of the offered incentives in Experiment I for 7-8 AM

Experiment I, Time: 7-8 AM						
Budget	Incentive					
	$0	$1	$2	$5	$10	$1000
$1,000	6740	324	338	0	0	0
$10,000	4210	275	1620	1297	0	0

Table 31: Distribution of the offered incentives in Experiment I for 8-9 AM

Experiment I, Time: 8-9 AM						
Budget	Incentive					
	$0	$1	$2	$5	$10	$1000
$1,000	5751	258	371	0	0	0
$10,000	3352	199	1448	1381	9	0

Table 32: Distribution of the offered incentives in Experiment II for 7-8 AM

Experiment II, Time: 7-8 AM			
Budget	Incentive		
	$0	$2	$10
$1,000	4356	500	0
$10,000	1016	3550	290

Table 33: Distribution of the offered incentives in Experiment II for 8-9 AM

Experiment II, Time: 8-9 AM			
Budget	Incentive		
	$0	$2	$10
$1,000	3808	500	0
$10,000	876	3040	392

Table 34: Distribution of the offered incentives in Experiment III for 7-8 AM

Experiment III, Time: 7-8 AM						
Budget	Incentive					
	$0	$1	$2	$5	$10	$1000
$1,000	14525	349	153	69	0	0
$10,000	11789	945	1255	905	202	0

Table 35: Distribution of the offered incentives in Experiment III for 8-9 AM

Experiment III, Time: 8-9 AM						
Budget	Incentive					
	$0	$1	$2	$5	$10	$1000
$1,000	13071	135	140	117	0	0
$10,000	10319	785	1215	931	213	0

Table 36: Distribution of the offered incentives in Experiment IV for 7-8 AM

Experiment IV, Time: 7-8 AM			
Budget	Incentive		
	$0	$2	$10
$1,000	14641	440	12
$10,000	11877	2770	446

Table 37: Distribution of the offered incentives in Experiment IV for 8-9 AM

Experiment IV, Time: 8-9 AM			
Budget	Incentive		
	$0	$2	$10
$1,000	13077	355	29
$10,000	10609	2315	537